약학석사 학위논문

Coumarins and Biflavonoids from *Edgeworthia chrysantha* and Their Glucose Uptake Activity

삼지닥나무에서 분리된 Coumarin 및 Biflavonoid 성분과 Glucose Uptake Activity

2020년 2월

서울대학교 대학원

약학과 생약학 전공

한 소 희

Coumarins and Biflavonoids from *Edgeworthia chrysantha* and Their Glucose Uptake Activity

삼지닥나무에서 분리된 Coumarin 및 Biflavonoid 성분과 Glucose Uptake Activity

지도 교수 오 원 근

이 논문을 약학석사 학위논문으로 제출함
2020 년 2 월

서울대학교 대학원
약학과 생약학전공
한 소 희

한소희의 약학석사 학위논문을 인준함
2019 년 2 월

위 원 장 _____ (인)

부위원장 _____ (인)

위 원 _____ (인)

Abstract

Edgeworthia chrysantha Lindl., also known as *Edgeworthia papyrifera* S. et Z., belongs to the *Edgeworthia* genus of the family Thymelaeaceae. It is a deciduous suckering shrub that inhabits forests and bushy slopes in Southwest China and has been cultivated throughout China, Japan and Korea. Traditionally, its stems and barks were used for making papers and for treating rheumatism in the folk medicine, respectively. Phytochemical and pharmacological studies of *E. chrysantha* have revealed that it comprises a variety of oligophenolic components such as coumarins, flavonoids and biflavonoids. It has been reported that the coumarins and their glycosides demonstrated anti-inflammatory and analgesic effects as well as α-glucosidase and α-amylase inhibitory activities. However, not much research was conducted on the roots of *E. chrysantha*. In the present study, nine compounds, including four dicoumarins (**1–4**), two tricoumarins (**5–6**), and three biflavonoids (**7–9**), were isolated from the roots of *E. chrysantha.* Among the isolated compounds, 6″-*O*-(3-hydroxy-3-methylglutaryl)-daphneretusin A (**1**) is reported from nature for the first time. Known compounds **2**–**3** and **6–9** have not yet been reported from *E. chrysantha*. All nine compounds were tested for their glucose uptake activity in 3T3-L1 adipocytes, and the results showed that compound **1** most effectively increased 2-NBDG uptake into 3T3-L1 adipocytes.

Keyword: *Edworthia chrysantha*, Thymelaeaceae, coumarins, biflavonoids, glucose uptake

Student Number: 2019-20085

Table of Contents

List of Abbreviations

$[\alpha]_D$: specific rotation

api: apiose

n-BuOH: *n*-butanol

calcd: calculated for MS analysis

CD: circular dichroism

DMSO: dimethyl sulfoxide

δ: chemical shift (ppm)

d: doublet

dd: doublet of doublet

glc: glucose

HMBC: heteronuclear multi-bond correlation

H_2O: water

HPLC: high performance liquid chromatography

HRESIMS: high-resolution electrospray ionization mass spectrometry

HSQC: heteronuclear single quantum coherence

HMG: 3-hydroxyl-e-methyl glutaroyl moiety

Hz: hertz

hr: hour

J: coupling constant in NMR

λ_{max}: max UV-vis wavelength

LC-MS: liquid chromatography-mass spectrometry

MeCN: acetonitrile

m: multiplet

CH_3OH: methanol

MS: mass spectrometry

2-NDBG: 2-(*N*-(7-Nitrobenz-2-oxa-1,3-diazol-4-yl)Amino)-2-

Deoxyglucose

NMR: nuclear magnetic resonance

OMe: methoxy group

q: quartet

RP: reverse phase

s: singlet

t: triplet

TLC: thin layer chromatography

UV: ultraviolet absorption spectroscopy

List of Figures

List of Tables

List of Schemes

I. Introduction

1.1. *Edgeworthia chrysantha* Lindl. (Thymelaeaceae)

The family Thymelaeaceae constitutes about 48 genera and 650 species. *Edgeworthia chrysantha* Lindl., also known as *Edgeworthia papyrifera* S. et Z., is one of the five species stemming from the *Edgeworthia* genus of the family Thymelaeaceae (eFloras 2008). It is a deciduous suckering shrub that inhabits forests and bushy slopes in Southwest China and has been cultivated throughout China, Japan and Korea (Clennett et al. 2002). Traditionally, stout and fibrous stems were used as ingredients for making papers called *washi* in Japan (Hughes 1978), while in China, its barks were used in the folkloric medicine for tendon relaxation and treating rheumatism. The fragrant and pilose clusters of yellow-white flowers were used as crude drugs for the treatment of ophthalmalgia and delacrimation as well as a decorative piece in the garden for their ethereal beauty (Li et al. 2014; Tong et al. 2009).

Phytochemical and pharmacological studies of the *Edgeworthia* genus have revealed that it comprises a variety of oligophenolic components such as coumarins of various skeletal patterns (Li et al. 2014; Hu et al. 2009; Baba et al. 1990, 1989; Chakrabarti et al. 1986; Majumder et al. 1974), flavonoids (Tong et al. 2009; Zhang et al. 1997) and biflavonoids (Zhou et al. 2010). Less commonly, sterols (Hashimoto et al. 1991) have been isolated from this genus. It has been reported that the coumarins and their glycosides exhibited anti-inflammatory and analgesic effects (Hu et al. 2008) as well as α-glucosidase and α-amylase inhibitory activities (Zhou et al. 2015). The flower of *Edgeworthia gardneri* (Wall.) Meisn.

showed anti-diabetic activity (Zhuang et al. 2018), anti-adipogenesis effects (Gao et al. 2016), anti-hyperglycemic activity (Ma et al. 2015), a PPAR activity (Xu et al. 2012) and polymerase β lyase inhibition effect (Li et al. 2004). Much of the aforementioned research was conducted on the flower and aerial parts of the plant. Not much phytochemical or pharmacological research has been done on the roots of *E. chrysantha*, however (Figure 1).

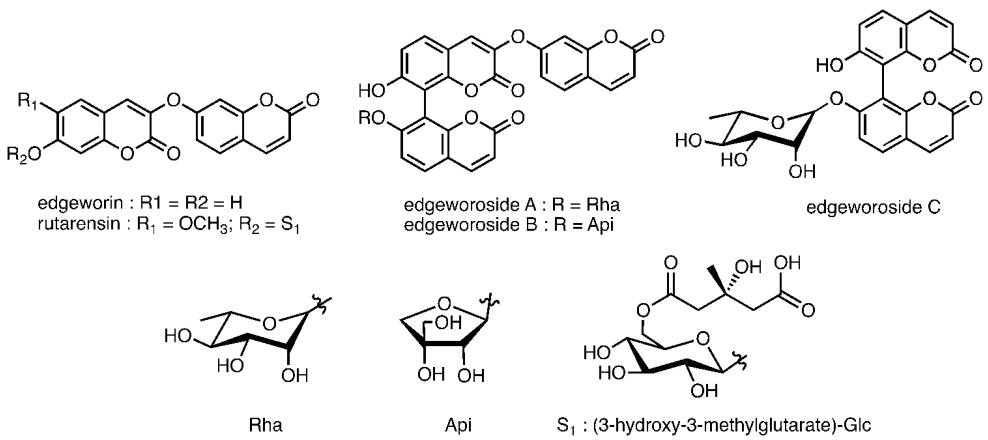

Figure 1. Reported compounds from *Edgeworthia chrysantha* roots

1.2. Coumarins

Coumarin, first isolated in 1822 from the tonka bean–*Dipteryx odorata*–is present in a myriad natural products, including tonka beans, cassia oils, sweet clover, and lavender. The structure of the coumarins is benzene fused with a α-pyrone ring, namely a 2*H*-chromen-2-one (1,2-benzopyrone) oxa-heterocycle. They can be found as free forms but often appear as conjugated to sugars and acids in families such as the Thymeleaceae, Umbelliferae and Rutaceae (Dewick 2009).

Biosynthetically, the formation of the coumarins in nature is enzymatically-derived. It originates from the phenylpropanoid pathway, in which

cinnamic acid hydroxylates at the ortho position of the side-chain. The 2-hydroxycinnamic acids then undergo *trans-cis* isomerization, while the newly established conformation is stabilized by the fully conjugated system (Dewick 2001) (Figure 2). Consequentially, chemical lactonization results in the formation of the coumarin monomer and umbelliferone. The additional hydroxylation occurs meta to the existing hydroxyl group on the aromatic ring resulting in other modified coumarins.

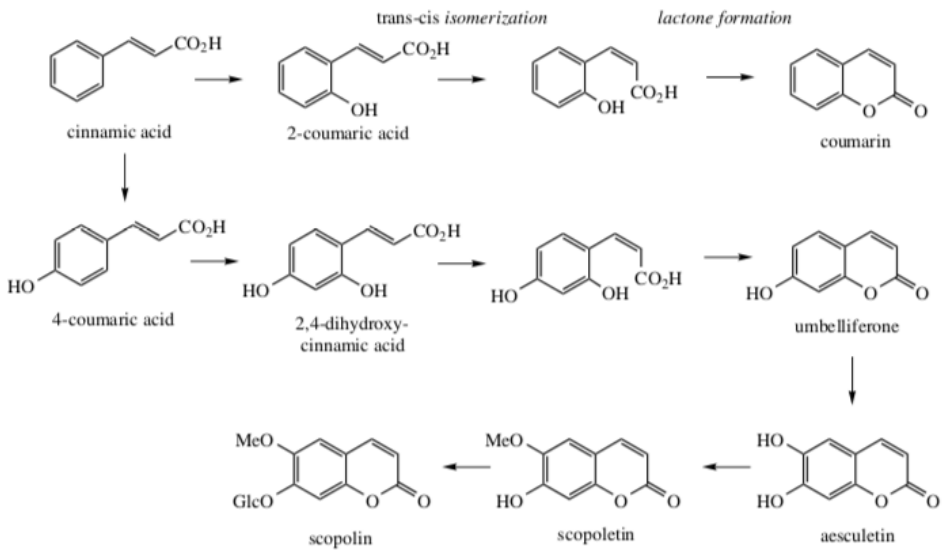

Figure 2. Biosynthesis of monomeric coumarins (Dewick 2001)

The simple coumarin monomers increase their structural complexity by forming into the dimeric and trimeric molecules. Such diversification occurs through an intrinsic reactivity of the simpler precursor structures as self-construction mechanisms (Gravel & Poupon 2008). There is a growing interest in these oligomers because the relative positioning of the functional groups may potentially provide chemical space and their possible efficacy for future clinical medicine unlike the synthetic counterparts. As an example, coumarin dimers and

trimers featuring C–C or C–O–C ether biaryl linkages are known to exhibit anti-diabetic, anti-inflammatory and anti-viral activities as well as an inhibitory activity against α-glucosidase (Menezes & Diederich 2019). The first tricoumarin reported in the literature, wikstrosin, was isolated from *Wikstroemia viridiflora*, belonging to Thymelaeaceae, the family *E. chrysantha* is part of. Other trimeric coumarins have been isolated in conjunction with a rhamnosyl and apiosyl sugar units with different glycosylation sites (Kreher et al. 1990).

Thus far, the known efficacy of coumarin-type compounds is as anticoagulant, tumoristatic, anti-inflammatory agents. Coumarin-type compounds are also known as a remedy to treat bruises and other skin diseases (Dewick 2009). It is of importance to note that coumarins are natural products whose metabolism and toxicity vary in species. According to an assessment regarding the coumarin toxicity, coumarin metabolism, in which coumarins are metabolized to 7-hydroxycoumarins in man, is a detoxification pathway and that coumarin present in food and cosmetics is negligible (Lake et al., 1999).

1.3. Biflavonoids

Biflavonoids are a subclass of flavonoids first isolated from *Ginkgo biloba* L. in 1929 and have been isolated from plants since (Gontijo et al. 2017). Presumably, they are considered oxidation products of naringenin chalcone where the condensation step results in dimeric structures. Several variations occur such as the positional difference in the interflavonoid linkage, hydroxyl/methyl substitutions and glycosylation patterns. The oxidation state of the heterocyclic ring also varies, but the most commonly known biflavonoids often contain the

carbonyl group (Geiger & Quinn 1988).

According to Geiger and Quinn, biflavonoids are separated into three main groups–biflavones, flavanone-flavone, and biflavanones. Different combinations of flavanone, flavone, flavonol and other flavonoid monomers are possible, however, leading to the vast structural diversity. The linkage between flavonoid monomers can either be by a C-C bond or a C-O-C ether bond (Kim et al. 2008). Structures of the most studied biflavonoids with 3′ → 8″, 3 → 8″, 3′ → 6″, 4′-O-6″, and 5′ → 4‴ linkage are as follows (Gontijo et al. 2017) (figure 3).

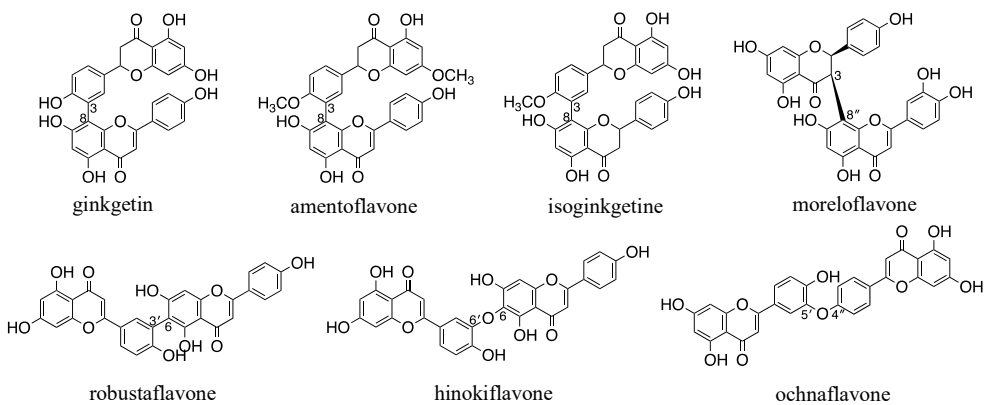

Figure 3. Structures of most studied biflavonoids (Gontijo et al. 2017)

Other flavonoid oligomers, similar to the primitive definition of the biflavonoids, are the proanthocyanidins. The main difference between the two kinds of dimers is while the biflavonoids comprise the carbonyl group, the proanthocyanidins contain flavanones that have been reduced. Moreover, the interflavonoid linkages in the proanthocyanidins occur in position 4 of the upper unit and 6 or 8 of the lower unit (Geiger & Quinn 1988).

Naturally occurring biflavonoids are known to contain diverse pharmacological activities such as antibacterial, antifungal, anti-inflammatory,

antiviral effects, etc (Kim et al. 2008). According to a study, biflavonoids isolated from the roots of *Wikstroemia indica* (Linn.) C.A. Mey., belonging to the Thymelaeaceae family, exhibited an *in vitro* antiviral activity against human Respiratory Syncytial Virus (RSV) (Gontijo et al. 2017). Due to their chemical diversity, numerous pharmacological properties, and their abundance in nature, biflavonoids pose as plant secondary metabolites with potential for drug development.

1.4. Diabetes

According to estimates by World Health Organization, the severity of the emerging diabetes epidemic continues to rise. In 2016, the number of adults reportedly suffering from diabetes was 422 million, the number equivalent to 1 in 11 individuals (WHO 2016). Diabetes mellitus (DM) is a metabolic disease characterized by persistently high glucose levels in the blood called hyperglycemia. In a properly functioning body, glucose in the bloodstream gets inside the cells and provides the body with energy. Such glucose transport into the cell is stimulated by the hormone insulin secreted by the pancreas when the blood glucose level is high. Insulin then binds to the insulin receptor, from which a series of signaling cascade occurs and ultimately results in translocation of GLUT4 vesicles toward the plasma membrane (Figure 4). In essence, insulin deficiency by defective insulin secretion and/or the body's abnormal response to insulin action characterize diabetes (American Diabetes Association 2010).

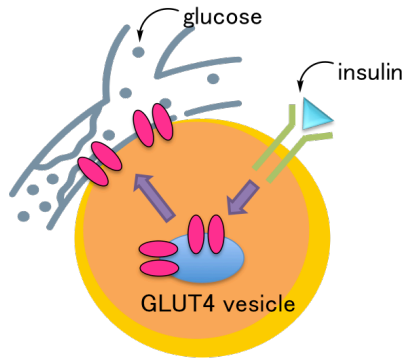

Figure 4. Insulin signaling and glucose transport in adipocyte

There are several types of diabetes mellitus. Among them, type-I and type-II DM are most common. Type-I diabetes occurs as an autoimmune disease in which the body fails to produce insulin. This type is incurable and unpreventable but can be managed by taking insulin and regulating sugar intake. Type-II diabetes is caused by insulin resistance of the cells and body's inadequate response to the hormone. Also known as adult-onset diabetes, obesity increases the risk of type-II diabetes.

There are a variety of drugs for the treatment of type-I and type-II diabetes currently available on the market; however, new agents are subject to a continuous effort in development due to a great health threat associated with diabetes and its high prevalence (Levien & Baker 2009). Despite the significant progress made in the treatment of diabetes, medicinal plants have gained popularity to combat the inevitable disadvantages of synthetic anti-diabetic drugs, i.e., side effects, resistance, and toxicity (Kooti et al. 2016). A number of plants have been reviewed and evaluated for their anti-diabetic effect, but there needs more research to find the active components from plants and study their curative properties.

II. Materials and Methods

2.1. Plant materials

The whole plant of *Edgeworthia chrysantha* Lindl. was collected at Medicinal Plant Garden (The College of Pharmacy, Seoul National University, Goyang-si, Gyeonggi-do, Korea). The sample was identified by Sang-il Han (Medicinal Plant Garden, College of Pharmacy, Seoul National University).


2.2. Reagents and equipment

2.2.1. Chemical reagents

- Formic acid (Sigma-Aldrich, MO, USA)
- HPLC grade solvent: MeCN and MeOH (HoneyWell Burdick & Jackson®, MI, USA)
- NMR solvents: methanol-d_4 and DMSO-d_6 (Cambridge Isotope Laboratories, Inc., MA, USA)
- MPLC cartridge: Watchers® Flash RP18; particle size 40-60 μm (ISU Industry Corp., Seoul, Republic of Korea)

- Normal-phase silica gel: ZEOprep®; pore size 60 Å; particle size 40-63 μm (Zeochem AG, Uetikon am See, Switzerland)
- Sephadex TM LH-20; bead size 25-100 μm (GE Healthcare, IL, USA)
- Solvents used for extraction, fraction and isolation: n-Hexane, EtOAc, aceone, MeOH, n-BuOH; analytical grade (Daejung Pure chemical Eng. Co. Ltd., Si-heung, Republic of Korea)
- TLC Silicagel 60 F254 (Art. 15389, Merck, Germany)
- TLC Silicagel 60 C-18 F254 (Art. 15389, Merck, Germany)
- TLC visualization reagent: 10 % H2SO4 in EtOH

2.2.2. Bioassay reagents

- Dexamethasone (Sigma, MO, USA)
- DMSO: dimethyl sulfoxide (Junsei Chemical Co. Ltd., Tokyo, Japan)
- Dulbecco's modified Eagle's Medium (DMEM) (Introgen, CA, USA)
- FBS: fetal bovine serum (HyClone, UT, USA)
- Insulin (Roche, Mannheim, Germany)
- 3-isobutyl-1-methyl-xanthine (Sigma, MO, USA)
- 2-NBDG: 2-[N-(7-nitrobenz-2-oxa-1,3-diazol-4-yl)amino]-2-deoxy-d-glucose (Invitrogen, CA, USA)
- Reagents for cell differentiation (Gibco, NY, USA)

    Calf serum

    Penicillin; 100 U/mL

    Streptomycin; 100 μg/mL

- MTT reagent (Sigma, MO, USA)

- PBS: phosphate-buffered saline (Takara, Shiga, Japan)

2.1.3. Experimental instruments

- Analytical balance: Sartorius BSA 2245-CW; max 220 g, d = 0.1 mg (Sartorius, Goettingen, Germany)
- Autoclave: LAC-5080S (Daihan Science, Seoul, Korea)
- Clean bench: Class II biological safety cabinet (Esco Technologies, Inc., PA, USA)
- CO_2 incubator: Forma™ series II water-jacketed (Thermo Fisher Scientific Inc., MA, USA)
- Fluorescence microplate reader: Spectra Max Gemini XPS (Molecular Devices, CA, USA)
- Fluorescence microscope: Olympus ix70 (Olympus Co., Tokyo, Japan)
- LC-MS system: Agilent HPLC 6130 spectrometer equipped with 1260 Infinity system (Agilent Technologies, CA, USA)
- NMR spectrometers

  JEOL JMN-ECZ400s Spectrometer; 400 MHz (JEOL Ltd., Tokyo, Japan)

  Bruker Avance 500 Spectrometer; 500 MHz (Bruker, Germany)

  JEOL JMN-ECA600 Spectrometer; 600 MHz (JEOL Ltd., Tokyo, Japan)
- Polarimeter: Jasco P-2000 polarimeter (Jasco, Japan)
- Rotary evaporator: EYELA KSB-202 (Tokyo Rikakikai Co., Ltd., Tokyo, Japan)
- Ultrasonicator: Powersonic 420 (Hwashin Technology, Seoul, Korea)
- Analytical HPLC system and column:

  Dionex UltiMate 3000 (Thermo Scientific Inc., MA, USA)

YMC-Triart C18; 4.6 x 250 mm (YMC Co. Ltd., Tokyo Japan)

- MPLC system and column:

Biostage Isolera™ (Biostage, Inc., MA, USA)

Watchers®flash cartridge C18; 120 g; column (ISU Industry Co., Seoul, Korea)

2.3. Isolation of chemical constituents from *E. chrysantha* roots

2.3.1. Extraction and fractionation

The air-dried roots of *Edgeworthia chrysantha* (380 g) was pulverized and extracted three times by sonication with 1.2 L of 90% ethanol for 90 min each. The extract was filtered and concentrated *in vacuo*. The residue (28 g) was sequentially fractionated with *n*-hexane (3 x 1 L), EtOAc (3 x 1 L), *n*-BuOH (3 x 1 L) and H_2O. The solvent was removed under reduced pressure. The EtOAc fraction weighed 5 g with a yield of 17.9 %.

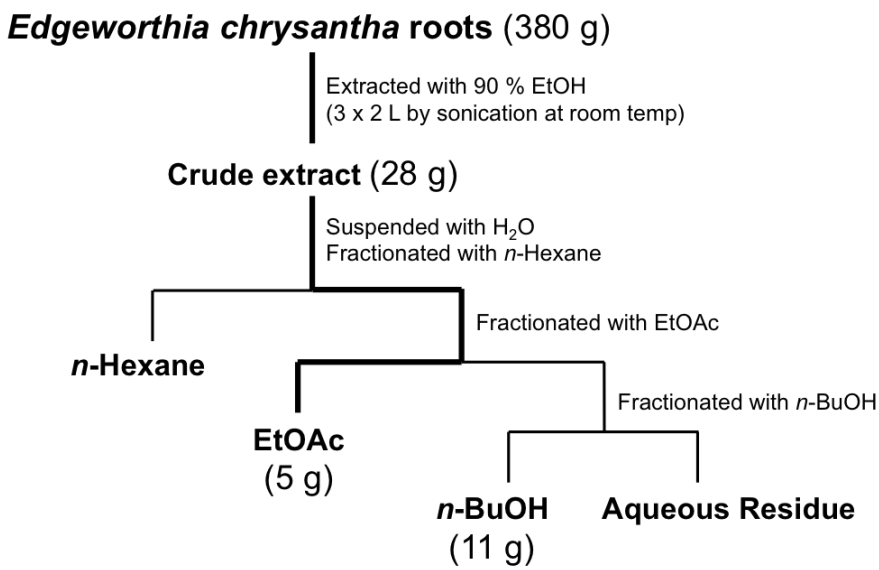

Scheme 1. Extraction and fractionation of *E. chrysantha* roots

2.3.2. Isolation of chemical constituents from the EtOAc fraction

The EtOAc fraction (5.0 g, yield: 17.9 %) was subjected to further fractionation by MPLC (ISU-C18 120 g, flow rate 20 mL/min, UV 254 nm and 360 nm detection) with a gradient mixture of MeOH and H_2O containing 0.1 % formic acid (10:90 → 80:20) over 60 min. Separation resulted in total of 12 fractions (1–12), which were combined based on TLC patterns. Fraction 9 (648.6 mg) was subjected to further separation by sephadex LH-20 with 100 % MeOH as the mobile phase in the isocratic system and divided into eight subfractions (9.1–9.8). Semipreparative HPLC was performed on subfraction 9.3 (286.5 mg) using a YMC-Triart Phenyl column in the isocratic system (MeCN:H_2O, 28:72, flow rate of 4.0 mL/min, 55 min). As a result, compounds **1** (6.8 mg), **5** (5.1 mg), and **6** (2.3 mg) were isolated. Fraction 8 (854.8 mg) was subjected to sephadex LH-20 with 100 % MeOH in the isocratic system and yielded subfractions 8.1–8.5. Subfraction 8.3 (109.2 mg) was further chromatographed on semipreparative HPLC on a YMC-Triart Phenyl column (MeOH:H_2O, 40:60, flow rate 4.0 mL/min, 60 min) and afforded a dicoumarinyl ether glucoside (**2**, 5.3 mg). Subfraction 8.4 (331.7 mg) was submitted to semipreparative RP-HPLC on a YMC-Triart C18 (MeCN:H_2O, 21:79, flow rate 3.9 mL/min, 50 min), from which biflavonoids **7** (8.2 mg), **8** (6.7 mg), and **9** (5.9 mg) were isolated. Compound **3** (22.0 mg) was provided from fraction 12 (370.0 mg), which was first separated by sephadex LH-20 with 100 % MeOH in the isocratic system. Fraction 7 (483.1 mg) was applied to sephadex LH-20 with the isocratic mobile system with 100 % MeOH. Subfraction 2 (88.6 mg) was further purified by RP-HPLC (MeOH:H_2O, 53:47) and afforded compound **4** (4.2 mg). Fraction 10 (104.2 mg) was chromatographed by sephadex LH-20 with

100 % MeOH in the isocratic system. From subfractions 10.1–10.9 obtained, subfraction 10.4 (44.2 mg) was applied to semi semipreparative HPLC on a YMC-Triart Phenyl column (MeCN:H_2O, 25:60, flow rate 4.0 mL/min, 60 min). As a result, compound **5** (5.1 mg) was isolated.

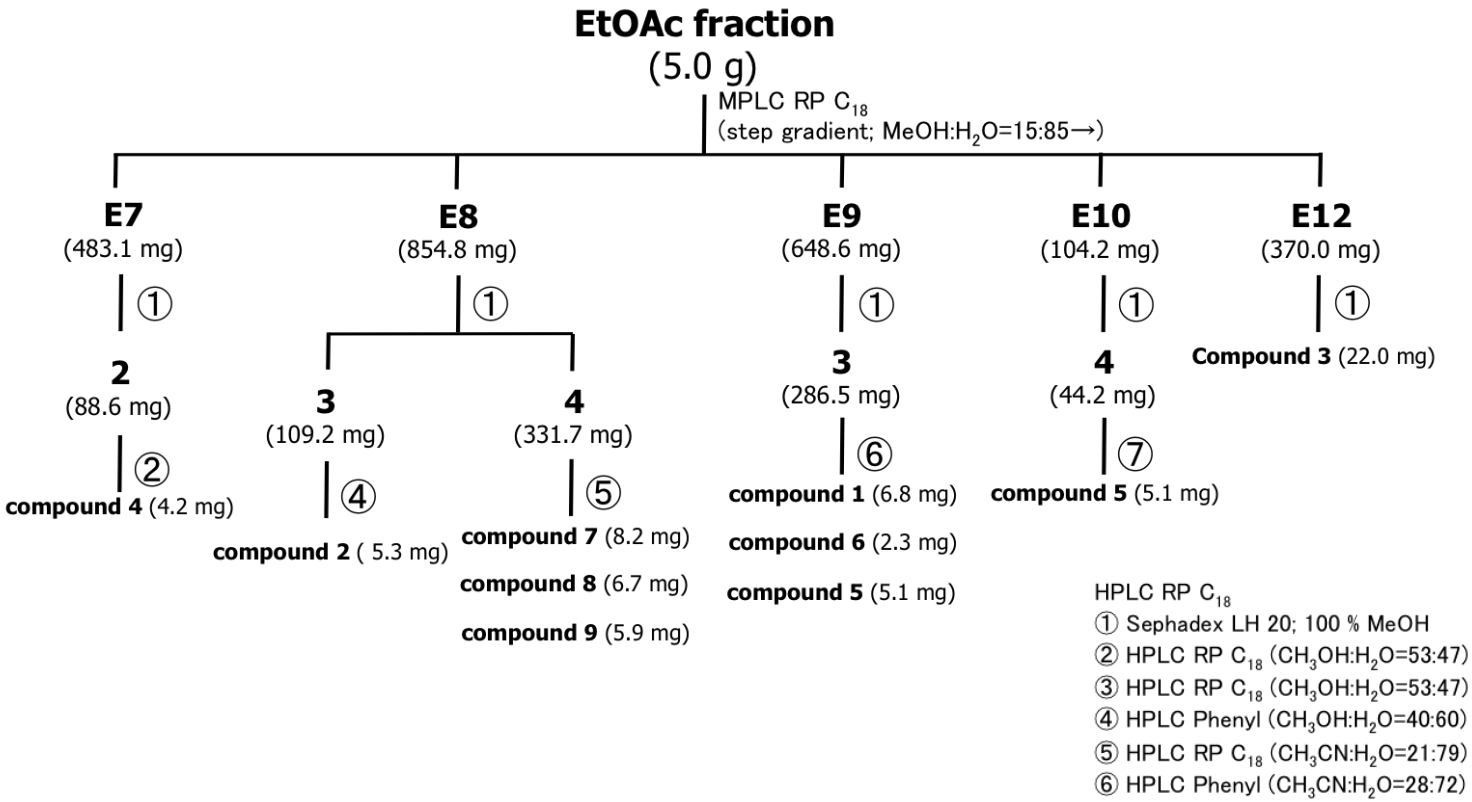

Scheme 2. Isolation of chemical constituents from the EtOAc fraction of *E. chrysantha* roots

2.3.3. Spectral data of isolated compounds

Compound **1**

6″-*O*-(3-hydroxy-3-methylglutaryl)-daphneretusin A

$[\alpha]_D^{20}$= -32.5° (c 0.5, MeOH)

Colorless amorphous powder

Blue fluorescence under UV

UV (MeOH) λmax (log ε) 263 (3.17), 338 (3.57) nm

ECD (MeOH) λmax (*Δε*) 216 (-1.32), 243 (-0.47), 284 (-0.10), 315 (-0.51), 341 (0.24), 359 (-0.40) nm

IR *υ*max 3340(-OH), 1730(-COO-), 1620, 1510, 1270 cm^{-1}

HRESIMS m/z 643.1299 $[M-H]^-$ (calcd for $C_{30}H_{27}O_{16}$, 643.1299)

^1H NMR (600 MHz, DMSO-d_6): Table 1

^{13}C NMR (150 MHz, DMSO-d_6): Table 2

Compound **2**

Daphneretusin A

Colorless amorphous powder

Blue fluorescence under UV

UV (MeOH) λmax (log ε) 338 (3.19) nm

ECD (MeOH) λmax ($\Delta\varepsilon$) 218 (-0.09), 250 (0.01) nm

HRESIMS m/z 499.0876 $[M-H]^-$ (calcd for $C_{24}H_{19}O_{12}$, 499.0877)

^{1}H NMR (600 MHz, DMSO-d_6): Table 1

^{13}C NMR (150 MHz, DMSO-d_6): Table 2

Compound **3**

Daphnoretin

Colorless amorphous powder

Blue fluorescence under UV

UV (MeOH) λmax (log ε) 286 (2.89), 324 (2.83), 337 (2.82) nm

ECD (MeOH) λmax ($\Delta\varepsilon$) 227 (-0.16), 279 (-0.11), 298 (-0.02), 333 (-0.06) nm

HRESIMS m/z 351.0529 $[M-H]^-$ (calcd for $C_{19}H_{11}O_7$, 351.0505)

^{1}H NMR (500 MHz, DMSO-d_6): Table 1

^{13}C NMR (125 MHz, DMSO-d_6): Table 2

Compound **4**

Edgeworoside C

Colorless amorphous powder

Blue fluorescence under UV

$[\alpha]_D^{20}$= -59.0° (c 0.08, MeOH)

UV (MeOH) λmax (log ε) 286 (2.89), 324 (2.83), 337 (2.82) nm

ECD (MeOH) λmax ($\Delta\varepsilon$) 227 (-0.16), 279 (-0.11), 298 (-0.02), 333 (-0.06) nm

HRESIMS m/z 467.0972 $[M-H]^-$ (calcd for $C_{24}H_{19}O_{10}$, 467.0978)

^{1}H NMR (600 MHz, DMSO-d_6): Table 3

^{13}C NMR (150 MHz, DMSO-d_6): Table 3

Compound **5**

Edgeworoside B

Colorless crystalline powder

Blue fluorescence under UV

$[\alpha]_D^{20}$= -96.2° (c 0.1, MeOH)

UV (MeOH) λmax (log ε) 207 (3.69), 325 (3.49) nm

ECD (MeOH) λmax ($\Delta\varepsilon$) 214 (-1.08), 226 (2.79), 312 (-1.46), 344 (3.17) nm

HRESIMS m/z 613.0980 $[M-H]^-$ (calc. for C32H21O13, 613.0982)

^{1}H NMR (600 MHz, DMSO-d_6): Table 4

^{13}C NMR (150 MHz, DMSO-d_6): Table 4

Compound **6**

7''-*O*-(β-D-glucopyranosyl)-triumbelletin

Pale yellow amorphous powder

$[\alpha]_D^{20}$= 30.9° (c 0.2, MeOH)

UV (MeOH) λmax (log ε) 325 (3.59) nm

ECD (MeOH) λmax ($\Delta\varepsilon$) 206 (-5.06), 226 (5.10), 310 (-2.51), 342 (6.41) nm

HRESIMS m/z 643.1085 $[M-H]^-$ (calcd for $C_{33}H_{23}O_{14}$, 643.1088)

^{1}H NMR (600 MHz, DMSO-d_6): Table 2

^{13}C NMR (150 MHz, DMSO-d_6): Table 2

Compound **7**

Daphnodorin I

Pale yellow amorphous powder

$[\alpha]_D^{20}$= -265.6° (c 1.0, MeOH)

UV (MeOH) λmax (log ε) 216 (3.22), 286 (2.75) nm

ECD (MeOH) λmax ($\Delta\varepsilon$) 204 (1.05), 229 (-1.30), 280 (-0.73), 331 (-0.61) nm

HRESIMS m/z 541.1159 $[M-H]^-$ (calcd for $C_{30}H_{21}O_{10}$, 541.1135)

^{1}H NMR (500 MHz, MeOD-d_4): Table 5

^{13}C NMR (125 MHz, MeOD-d_4): Table 5

Compound **8**

Wikstrol A

Pale yellow amorphous powder

$[\alpha]_D^{20}$= -31.2° (c 1.0, MeOH)

UV (MeOH) λmax (log ε) 207 (4.05), 266 (3.71), 331 (3.38) nm

ECD (MeOH) λmax ($\Delta\varepsilon$) 226 (-1.63), 241 (-0.02) nm

HRESIMS m/z 541.1157 $[M-H]^-$ (calcd for $C_{30}H_{21}O_{10}$, 541.1135)

^{1}H NMR (400 MHz, MeOD-d_4): Table 6

^{13}C NMR (100 MHz, MeOD-d_4): Table 6

Compound **9**

Wikstrol B

Pale yellow amorphous powder

$[\alpha]_D^{20}$= -13.6° (c 1.0, MeOH)

UV (MeOH) λmax (log ε) 210 (3.65), 266 (3.32), 333 (3.05) nm

ECD (MeOH) λmax ($\Delta\varepsilon$) 226 (-0.49), 240 (-1.81) nm

HRESIMS m/z 541.1135 $[M-H]^-$ (calcd for $C_{30}H_{21}O_{10}$, 541.1135)

^{1}H NMR (600 MHz, MeOD-d_4): Table 6

^{13}C NMR (150 MHz, MeOD-d_4): Table 6

Table 1. ^{1}H NMR spectral data of compounds **1**, **2**, and **3**

position	**1**[a]	**2**[a]	**3**[b]
	δ_H in ppm (integration, splitting pattern, *J*)		
2			
3			
4	7.88 (1H, s)	7.81 (1H, s)	7.88 (1H, s)
5	7.34 (1H, s)	7.37 (1H, s)	7.22 (1H, s)
6			
7			
8	6.91 (1H, s)	6.86 (1H, s)	6.87 (1H, s)
9			
10			
2′			
3′	6.37 (1H, d, 9.4)	6.37 (1H, d, 9.6)	6.38 (1H, d, 9.5)
4′	8.03 (1H, d, 9.6)	8.03 (1H, d, 9.6)	8.04 (1H, d, 9.6)
5′	7.70 (1H, d, 8.7)	7.70 (1H, d, 8.5)	7.71 (1H, d, 8.6)
6′	7.11 (1H, dd, 8.7, 2.4)	7.11 (1H, dd, 8.7, 2.4)	7.12 (1H, dd, 8.6, 2.5)
7′			
8′	7.19 (1H, d, 2.5)	7.18 (1H, d, 2.4)	7.19 (1H, d, 2.8)
9′			
10′			
Glc			
1″	4.83 (1H, d, 7.4)	4.74 (1H, d, 7.4)	
2″	3.36–3.28 (1H, m)	3.32–3.25 (1H, m)	
3″	3.36–3.28 (1H, m)	3.32–3.25 (1H, m)	
4″	3.22 (1H, m)	3.22–3.18 (1H, m)	
5″	3.59 (1H, ddd, 9.1, 6.3)	3.32–3.25 (1H, m)	
6″	4.37 (1H, dd, 11.9, 2.0)	3.71 (1H, dd, 11.9, 2.2)	
	4.05 (1H, dd, 11.9, 6.3)	3.50 (1H, dd, 11.9, 5.4)	
HMG			
1‴			
2‴	2.58 (1H, d, 14.2)		
	2.54 (1H, d, 14.2)		
3‴			
4‴	2.47 (1H, d, 15.0)		
	2.40 (1H, d, 14.8)		
5‴			
6‴			
6-OMe			3.81 (3H, s)

Recorded at [a]600 MHz and [b]500 MHz in DMSO-d_6.

Table 2. The ^{13}C NMR spectral data of compounds **1**, **2**, and **3**

position	**1**[a]	**2**[a]	**3**[b]
		δ_C in ppm	
2	156.9	157.0	157.0
3	135.8	135.3	135.7
4	131.0	131.1	130.9
5	114.2	114.8	109.4
6	142.9	143.4	145.7
7	148.5	152.2	150.3
8	103.2	103.2	102.8
9	150.7	148.8	147.4
10	110.4	109.7	110.2
2′	160.0	160.0	160.0
3′	113.8	113.8	113.9
4′	144.0	144.1	144.1
5′	129.9	129.9	129.9
6′	113.3	113.4	113.5
7′	159.7	159.8	159.7
8′	103.9	103.9	104.0
9′	155.0	155.0	155.0
10′	114.4	114.3	114.4
Glc			
1″	101.8	102.5	
2″	75.7	77.2	
3″	73.1	73.3	
4″	69.7	69.6	
5″	74.0	76.1	
6″	63.1	60.6	
HMG			
1‴	170.4		
2‴	45.1		
3‴	68.7		
4‴	45.3		
5‴	172.5		
6‴	27.5		
6-OMe			56.0

Recorded at [a]150 MHz and [b]125 MHz in DMSO-d_6.

Table 3. ^{1}H and ^{13}C NMR spectral data of compound **4**

position	**4**	
	δ_C	δ_H (integration, splitting pattern, *J*)
2	160.3	
3	110.7	6.18 (1H, d, 9.4)
4	144.7	8.01 (1H, d, 9.4)
5	129.2	7.61 (1H, d, 8.6)
6	112.8	7.00 (1H, d, 8.6)
7	159.7	
8	106.3	
9	153.2	
10	110.9	
2′	160.1	
3′	112.9	6.32 (1H, d, 9.6)
4′	145.0	8.08 (1H, d, 9.5)
5′	129.3	7.77 (1H, d, 8.7)
6′	111.3	7.30 (1H, d, 8.8)
7′	157.0	
8′	110.0	
9′	152.6	
10′	113.4	
Rha		
1″	98.4	5.47 (1H, s)
2″	70.0	3.43 (1H, m)
3″	70.1	3.03 (1H, dd, 9.4, 3.4)
4″	71.5	3.17 (1H, m)
5″	69.5	3.37 (1H, dd, 9.5, 6.1)
6″	17.8	1.06 (3H, d, 6.3)

Recorded at 600 MHz (δ_H) and 150 MHz (δ_C) in DMSO-d_6.

Table 4. ^{1}H and ^{13}C NMR spectral data of compound **5** and **6**

position	**5**		**6**	
	δ_C	δ_H	δ_C	δ_H
2	156.7		157.1	
3	134.9		133.2	
4	131.1	7.97 (1H, s)	131.2	7.95 (1H, s)
5	129.0	7.60 (1H, d, 8.6)	128.8	7.50 (1H, d, 8.6)
6	113.5	7.02 (1H, d, 8.5)	113.6	6.90–6.86 (1H, m)
7	159.0		159.9	
8	106.7		106.7	
9	151.1		151.6	
10	110.5		110.8	
2′	159.9		160.2	
3′	113.9	6.37 (1H, d, 9.6)	113.8	6.35 (1H, d, 9.5)
4′	144.0	8.03 (1H, d, 9.6)	144.1	8.02 (1H, d, 9.6)
5′	129.9	7.68 (1H, d, 8.7)	129.9	7.68 (1H, d, 8.6)
6′	113.2	7.09 (1H, dd, 8.5, 2.5)	113.5	7.04 (1H, dd, 8.5, 2.5)
7′	159.6		160.0	
8′	104.2	7.19 (1H, d, 2.5)	103.9	7.12 (1H, d, 2.2)
9′	155.0		155.0	
10′	114.4		114.3	
2″	160.2		162.3	
3″	112.8	6.32 (1H, d, 9.3)	112.9	6.32 (1H, d, 9.5)
4″	144.7	8.08 (1H, d, 9.6)	144.7	8.08 (1H, d, 9.5)
5″	129.2	7.77 (1H, d, 8.7)	128.9	7.75 (1H, d, 8.7)
6″	111.5	7.24 (1H, d, 8.7)	111.8	7.29 (1H, d, 8.7)
7″	157.6		158.4	
8″	109.9		108.7	
9″	152.6		152.5	
10″	113.2		113.0	

Table 4. (Continued)

position	**5**		**6**	
	δ_C	δ_H	δ_C	δ_H
Sugar				
1‴	107.2	5.64 (1H, d, 2.4)	101.2	5.01 (1H, d, 7.7)
2‴	76.4	3.77 (1H, d, 2.4)	77.1	3.36 (1H, m)
3‴	78.8		73.3	3.00 (1H, t, 8.3)
4‴	62.4	3.17 (1H, d, 11.2)	69.4	3.10 (1H, t, 9.3)
		3.13 (1H, d, 11.2)		
5‴	74.5	3.83 (1H, d, 9.5)	76.3	3.24 (1H, t, 8.9)
		3.64 (1H, d, 9.5)		
6‴			60.7	3.66 (1H, m)
				3.47–3.43 (1H, m)

Recorded at 600 MHz (δ_H) and 150 MHz (δ_C) in DMSO-d_6.

Table 5. ^{1}H and ^{13}C NMR spectral data of compound **7**

position	**7**	
	δ_C	δ_H (integration, splitting pattern, *J*)
2	82.2	4.57 (1H, d, 7.5)
3	68.7	3.83 (1H, td, 8.0, 5.5)
4	28.8	2.84 (1H, dd, 16.0, 5.0)
5	160.8	
6	90.7	6.11 (1H, s)
7	163.2	
8	103.5	
9	153.1	
10	102.5	
11	130.8	
12,16	128.8	6.70 (2H, d, 8.5)
13,15	115.8	7.06 (2H, d, 8.5)
14	157.8	
2′	92.8	5.67 (1H, d, 1.5)
3′	96.3	
4′	197.8	
5′	104.6	
6′	159.0	
7′	96.9	5.60 (1H, s)
8′	170.5	
9′	90.6	5.46 (1H, s)
10′	174.2	
11′	125.5	
12′, 16′	129.6	7.07 (2H, d, 8.5)
13′, 15′	115.7	6.69 (2H, d, 8.5)
14′	158.7	

Recorded at 600 MHz (δ_H) and 150 MHz (δ_C) in MeOD-d_4.

Table 6. ^{1}H and ^{13}C NMR spectral data of compound **8** and **9**

position	**8**[a]		**9**[b]	
	δ_C	δ_H	δ_C	δ_H
2	82.6	4.67 (1H, d, 6.0)	82.8	4.14 (1H, d, 8.0)
3	68.7	3.75 (1H, q, 6.2)	68.9	3.94—3.88 (1H, m)
4	27.3	2.66 (1H, dd, 16.2, 4.8)	29.0	2.87 (1H, dd, 16.0, 5.6)
5	157.8		157.8	
6	96.3	6.12 (1H, s)	96.5	6.05 (1H, s)
7	156.7		155.9	
8	100.2		100.6	
9	154.0		154.8	
10	100.7		101.5	
11	131.6		131.5	
12,16	128.7	6.68 (2H, d, 7.8)	129.5	7.10 (2H, d, 8.0)
13,15	115.9	6.56 (2H, d, 8.4)	115.8	6.71 (2H, d, 8.0)
14	158.0		158.9	
2′	164.7		165.2	
3′	114.1		114.2	
4′	183.8		183.7	
5′	163.3		163.3	
6′	99.8	6.19 (1H, d, 1.8)	99.7	6.20 (1H, s)
7′	165.7		165.5	
8′	94.5	6.37 (1H, s)	94.5	6.34 (1H, s)
9′	159.4		159.4	
10′	105.1		105.1	
11′	125.8		126.0	
12′, 16′	131.6	7.46 (2H, d, 9.0)	131.4	7.27 (2H, d, 8.4)
13′, 15′	115.9	6.75 (2H, d, 9.0)	115.6	6.67 (2H, d, 8.4)
14′	161.0		160.6	

Recorded at [a]400 MHz, [b]600 MHz (δ_H), and [a]100 MHz, [b]150 MHz (δ_C) in MeOD-d_4.

2.3.4. Sugar analysis

Compound **2** (2 mg) was reacted with 1N HCl (200 μL) and was heated in a water bath (90 °C). After 1.5 hours, the solution was neutralized using a saturated Na_2CO_3 solution. The result of hydrolysis was checked by TLC to detect the absence of the original spot. After the completion of the reaction, the thiocarbomoyl thiazolidine derivatives of the sample, D-(+)-glucose (1 mg) and L-(-)-glucose (1 mg) were prepared by adding L-cysteine methyl ester hydrochloroide (2 mg) and pyridine (200 μL). The mixture was reacted in the oven (60 °C) for 1 hour. *o*-Tolyl isothiocyanate (200 μL) was added to the reaction and was reacted for another 1 hour in the oven (60 °C) (Tanaka et al 2007).

The reaction mixtures were applied to analytical HPLC on a 250 x 4.6 mm i.d. YMC-Triart C18 column (YMC CO., Kyoto, Japan) at 35 °C with the isocratic 25 % acetonitrile as the solvent system (aqueous 0.1 % formic acid (A) and acetonitrile (B) for 30 min at the flow rate of 1 mL/min). The retention time of the thiocarbamoyl thiazolidine derivative of the sample at 21.1 min overlapped with that of D-(+)-glucose.

2.4. Evaluation of glucose uptake

2.4.1. Differentiation of 3T3-L1 cells into adipocytes

3T3-L1 preadipocytes were maintained in DMEM containing 10 % calf serum and penicillin(100 U/mL)–streptomycin(100 μg/mL) at 37 °C in an atmosphere of 5 % CO_2. Cells were grown until confluence and incubated for 2 days supplemented with 10 % FBS, 1 μg/mL insulin, 1 μM dexamethasone, and 520 μM 3-isobutyl-1-methyl-xanthine. The cells were continuously incubated and changed with fresh DMEM containing 10 % FBS, 1 μg/mL insulin, and penicillin(100 U/mL)–streptomycin(100 μg/mL) every 2 days. After adipogenic induction, the cells were incubated for additional 4 days and the lipid droplets were observed.

2.4.2. Evaluation of *in vitro* cytotoxicity in 3T3-L1 adipocytes

Evaluation of the viability of 3T3-L1 adipocytes was conducted by the MTT colorimetric assay. First, the cells were seeded into a 96-well microculture plate containing DMEM and 10 % FBS, and incubated at 37 °C in an atmosphere of 5 % CO_2 for 24 hours. After incubation, the cells were treated with the isolated compounds **1-9** in the serum-free medium and incubated for additional 24 hours. Afterwards, 20 μL of MTT solution (2 mg/mL) was added to each well and incubated in the dark for 4 hours. The medium was removed, and the precipitated formazan was dissolved in DMSO. The absorbance at 550 nm was measured with a microplate reader to measure the amount of viable cells after treatment with the tested compounds.

2.4.3. Evaluation of 2-NBDG uptake in 3T3-L1 adipocytes

Direct glucose uptake in 3T3-L1 adipocytes was monitored by 2-NBDG, which is a fluorescent D-glucose derivative. 3T3-L1 adipocytes were seeded into a 96-well microculture plate containing a glucose-free medium supplemented with 10 % FBS at 37 °C in an atmosphere of 5 % CO_2 for 24 hours. The cells were treated with the isolated compounds **1-9** and insulin as the positive control in the presence or absence of 2-NBDG. After 1 hour of incubation, the cultures were washed with PBS. The fluorescent intensity was measured with a fluorescence microplate reader at the excitation/emission wavelengths of 450/535 nm.

III. Results and Discussion

3.1. Structural elucidation of isolated compounds 1–9 from *E. chrysantha* roots

3.1.1. Compound 1

Compound **1** was isolated as a colorless amorphous powder. Its molecular formula was $C_{30}H_{28}O_{16}$ as deduced from the negative HRESIMS at *m/z* 643.1299 $[M-H]^-$ (calcd for $C_{30}H_{27}O_{16}$, 643.1299). From the UV spectrum showing absorption maxima at 338 (3.57) and 263 (3.17) [λ_{max} (log ε)] nm and the IR spectrum, which suggested the presence of hydroxyl groups at 3340 cm^{-1} and an *α,β*-unsaturated lactone at 1730 cm^{-1}, the presence of a coumarin derivative could be assumed.

In the ^1H NMR spectrum, a pair of doublet [δ_H 8.03 (1H, d, *J* = 9.6 Hz, H-4′) and 6.38 (1H, d, *J* = 9.0 Hz, H-3′)] corresponded to the signals that exhibited ortho coupling to each other. An ABX system [δ_H 7.70 (1H, d, *J* = 8.4 Hz, H-5′), 7.19 (1H, d, *J* = 3.0 Hz, H-8′), and 7.11 (1H, dd, *J* = 8.7, 2.4 Hz, H-6′)] and a lactone carbonyl group (–C=O) [δ_C 160.0 (C-2′)] in the ^{13}C NMR spectrum confirmed the presence of a benzopyran moiety. Additionally, the three aromatic proton signals [δ_H 7.88 (1H, s, H-4), 7.34 (1H, s, H-6) and 6.92 (1H, s, H-8)] and another carbonyl lactone [δ_C 156.9 (C-2)] belonged to a 3,6,7-trisubstituted coumarin moiety. The aforementioned signals and the rest of the quaternary carbon signals observed in the ^{13}C NMR spectrum were very similar to those of edgeworthin, which had been first isolated from *Edgeworthia gardneri* (Majumder et al. 1974);

thus, a linearly linked dimeric coumarin moiety was identified.

The anomeric proton signal at δ_H 4.83 (1H, d, J = 7.2 Hz, 1″) was assignable to the glucosyl moiety. Due to the coupling constant, the configuration of the anomeric proton was deduced to be the β-configuration. The rest of the proton signals shown at around δ_H 3.22–3.59 were assignable to the sugar moiety. Because the C-6″ glucose methylene protons [δ_H 4.37 (1H, d, J = 11.9, 2.0 Hz) and 4.05 (1H, d, J = 11.9, 6.3 Hz)] were shifted more downfield as compared to signals of an unsubstituted glucose moiety, an attachment of an ester group at this position could be deduced. Two pairs of doublet resonances [δ_H 2.40 (1H, d, J = 15.0 Hz, 2‴a)/2.47 (1H, d, J = 15.0 Hz, 2‴b), and 2.54 (1H, d, J = 13.8 Hz, 4‴a)/2.58 (1H, d, J = 7.2 Hz, 4‴b)] and the methyl protons [δ_H 1.16 (3H, s)] in conjunction with the carbon signals [δ_C 172.5 (C-5‴), 170.4 (C-1‴), 68.7 (C-3‴), 45.3 (C-4‴), 45.1 (C-2‴) and 27.5 (C-6‴) in the ^{13}C NMR spectrum suggested the presence of the 3-hydroxy-3-methylglutaryl (HMG) moiety.

The correlation signals observed from the HMBC experiment (Figure 6) confirmed the locations of glucose and HMG moieties. First, the correlation between H-1″ (δ_H 4.83) and C-6 (δ_C 142.9) linked glucose to the coumarin skeleton. Moreover, the cross-peak correlations seen between the H-6″ glucose methylene protons (δ_H 4.37 and 4.05) and HMG C-1‴ (δ_C 170.4) confirmed acylation at C-6″ hydroxyl of glucose.

The absolute configuration of the sugar unit was determined to be D-(+)-glucose by comparing the retention time of the thiocarbamoyl thiazolidine derivative of the sample with that of authentic D-(+)-glucose analyzed on RP-HPLC (Tanaka et al. 2007). Chirality at C-3 of the HMG moiety has not been established; however, the structure of 3-hydroxy-3-methylglutarate existing in

nature is derived through the acylation mechanism of HMG-CoA in the biosynthesis of the terpenoids (Hattori et al. 2007). Therefore, an *S*-configuration at this position is predicated. With the spectroscopic data, the structure of compound **1** was determined to be 6″-*O*-(3-hydroxy-3-methylglutaryl)-daphneretusin A, and it is reported from nature for the first time.

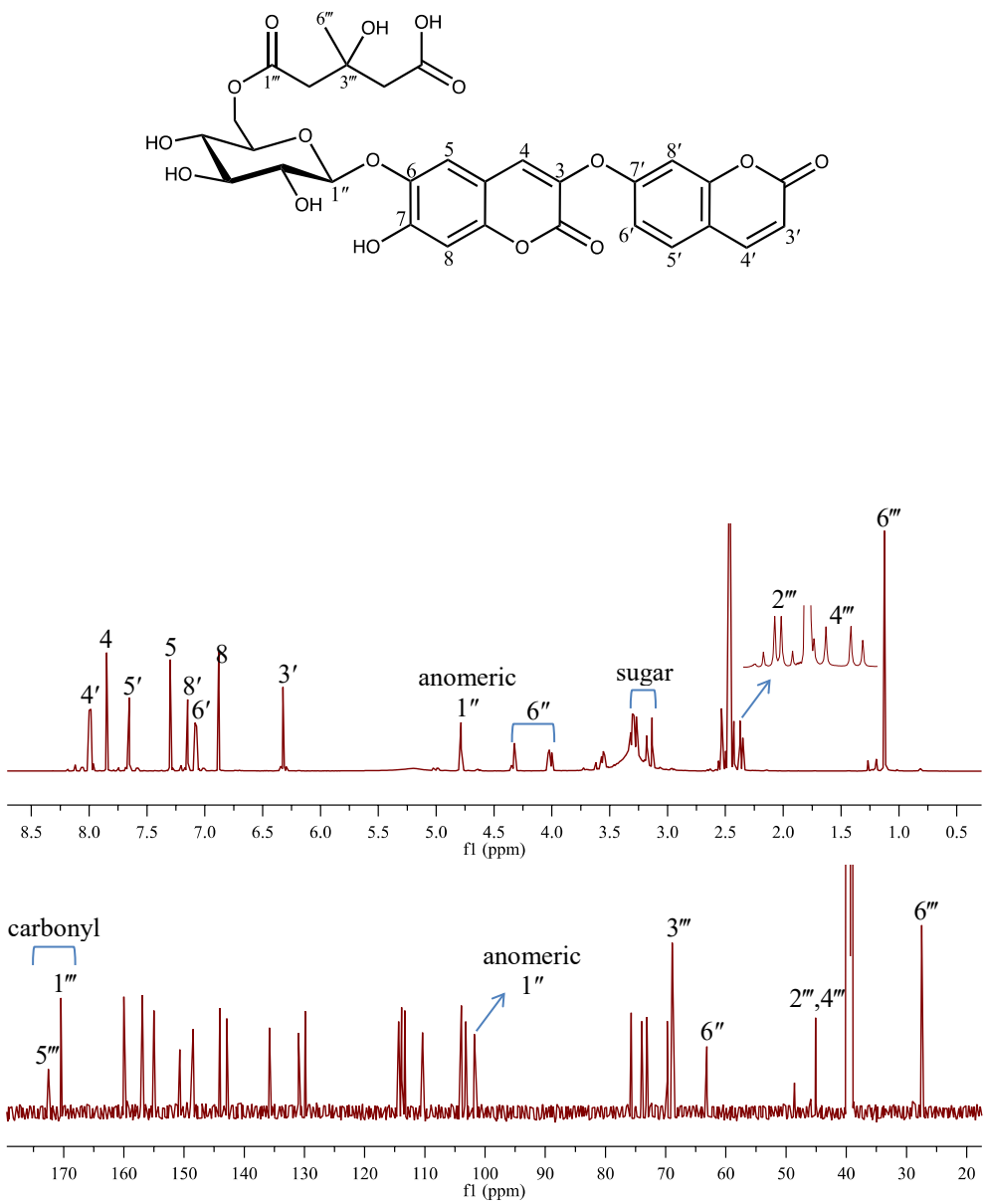

Figure 5. ^{1}H and ^{13}C NMR spectra of compound **1** in DMSO-d_6

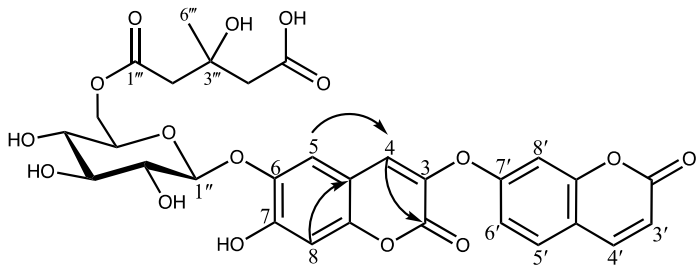

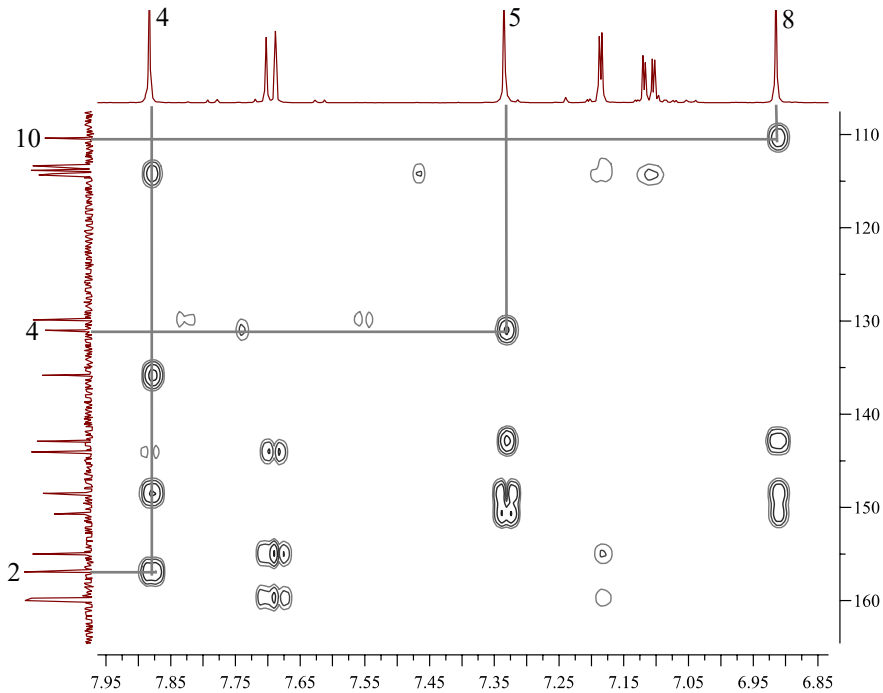

Figure 6. Key HMBC spectrum of compound **1**

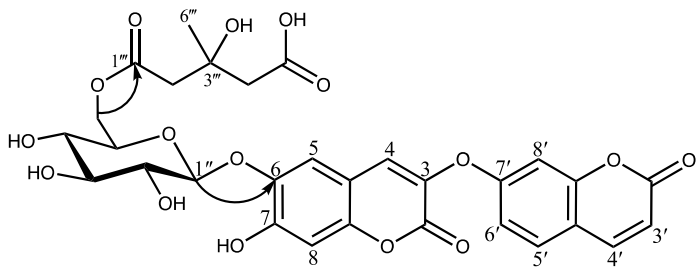

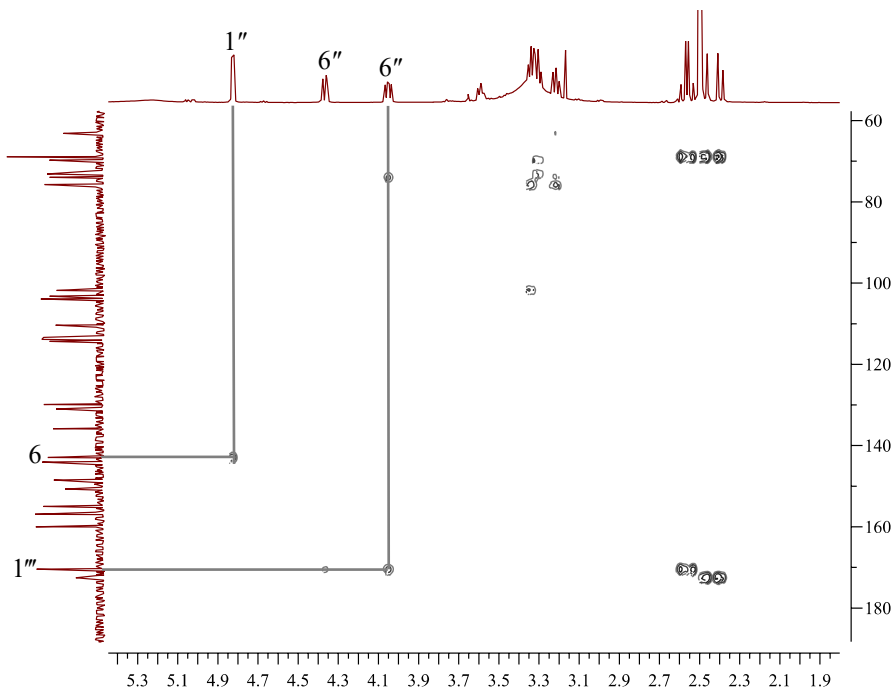

Figure 6. Key HMBC spectrum of compound **1** (continued)

3.1.2. Compound 2

Compound **2** was isolated as a colorless amorphous powder. Its empirical formula was confirmed as $C_{24}H_{20}O_{12}$ by the negative HRESIMS at *m/z* 499.0876 $[M-H]^-$ (calcd for $C_{24}H_{19}O_{12}$, 499.0877). The compound exhibited blue fluorescence on the TLC plate subjected to UV radiation at 365 nm. The diagnostic UV absorption bands were at 338 (319), 202 (3.61) [λ_{max} (log ε)] nm, suggesting a highly conjugated unsaturated system.

The ^{1}H NMR spectrum of compound **2** indicated the presence of a 7-coumarinyloxy group comprising a pair of doublets [δ_H 6.37 (1H, d, *J* = 9.6 Hz, H-3′) and 8.03 (1H, d, *J* = 9.6 Hz, H-4′)] and an ABX spin system [δ_H 7.70 (1H, d, *J* = 8.5 Hz, H-5′), 7.11 (1H, dd, *J* = 8.7, 2.4 Hz, H-6′) and 7.18 (1H, d, *J* = 2.4 Hz, H-8′)]. In conjunction with the three remaining singlet resonances [δ_H 7.81 (1H, s, H-4), 6.86 (1H, s, H-5) and 7.37 (1H, s, H-8)], the presence of a second 3,6,7-trioxygenated coumarin moiety similar to compound **1** could be deduced. The ^{1}H NMR spectrum also showed a doublet at δ_H 4.74 (1H, d, *J* = 7.4 Hz, H-1″), an anomeric signal characteristic of a sugar moiety. The configuration of the sugar unit was determined to be D by comparing the ^{1}H NMR and ^{13}C NMR chemical shifts as well as coupling constants with reference data (Pfeffer et al. 1979). The anomeric proton was further deduced to be β-oriented by the large coupling constant of 7.4 Hz. The ^{13}C NMR spectrum showed 23 carbon signals corresponding to the dimeric coumarin skeleton, including *α,β*-unsaturated carbonyl carbon atoms at δ_C 160.0 (C-2′) and 157.0 (C-2) and the signals assignable to the glucose moiety [δ_C 102.5, 77.2, 76.1, 73.3, 69.5 and 60.6].

The construction of the two coumarin monomers and the glucose moiety

was achieved by the correlation between the anomeric proton [δ_H 4.83 (H-1″)] and C-6 (δ_C 143.4) observed in the HMBC spectrum (Figure 9). Comparing the spectral data with those of the literature, compound **2** was determined to be daphneretusin A (Mansoor et al. 2013).

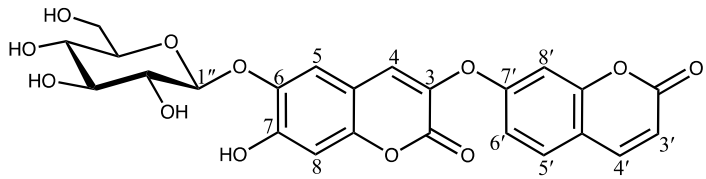

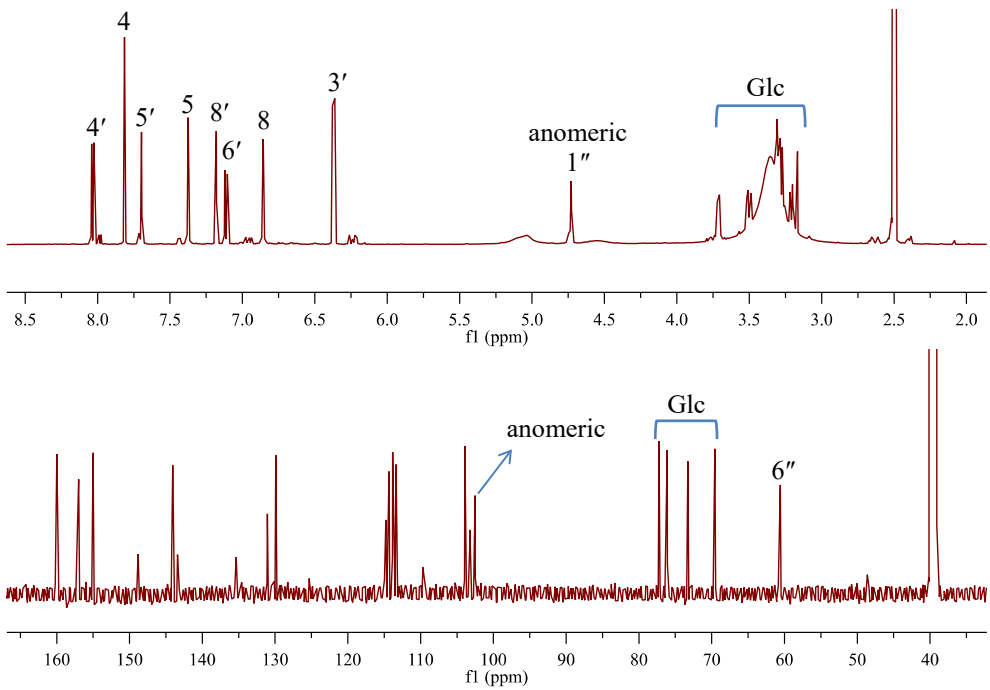

Figure 7. ^{1}H and ^{13}C NMR spectra of compound **2** in DMSO-d_6

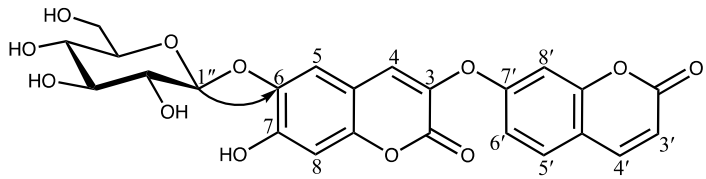

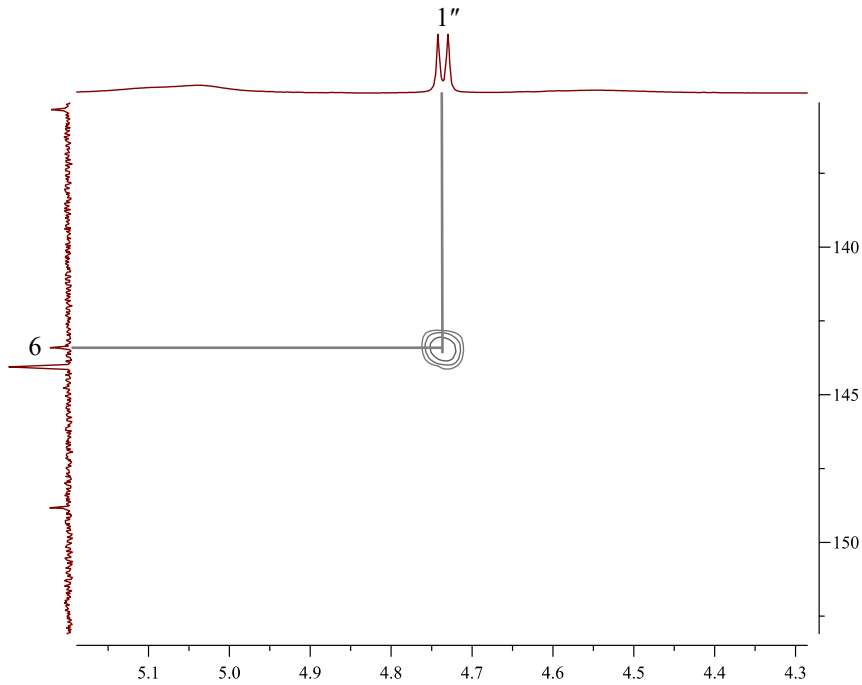

Figure 8. Key HMBC spectrum of compound **2**

3.1.3. Compound 3

Compound **3** was isolated as a colorless amorphous powder. Its molecular formula of $C_{19}H_{12}O_7$ was confirmed by the negative HRESIMS at *m/z* 351.0529 $[M-H]^-$ (calcd for $C_{19}H_{11}O_7$, 351.0505). The compound showed blue fluorescence on the TLC plate when visualized under the 365 nm UV light. The diagnostic UV absorption bands appeared at 337 (2.82), 324 (2.83), and 286 (2.89) [λ_{max} (log ε)] nm. The ^{1}H NMR spectrum of the compound showed two pairs of ortho coupled protons [δ_H 6.38 (1H, d, *J* = 9.5 Hz, H-3′) and 8.04 (1H, d, *J* = 9.6 Hz, H-4′), and 7.71 (1H, d, *J* = 8.6 Hz, H-5′) and 7.12 (1H, d, *J* = 8.6, 2.5 Hz, H-6′)], in which the latter pair forms an ABX spin system with the proton at δ_H 7.19 (1H, d, *J* = 2.8 Hz, H-8′). The remaining signals on the ^{1}H NMR spectrum revealed the presence of aromatic protons [δ_H 7.88 (1H, s, H-4), 7.22 (1H, s, H-5) and 6.87 (1H, s, H-8)] and a methoxy group [δ_H 3.81 (3H, s, 6-OMe)]. The ^{13}C NMR spectrum revealed 19 carbon atom signals, 18 of which were aromatic protons including methines, quaternary carbons and carbon atoms attached to oxygen, and 1 carbon signal corresponding to a methoxy carbon atom at δ_C 56.0. The ether linkage between C-3 (δ_C 135.7) and C-7′ (δ_C 157.0) was established by the chemical shifts of the neighboring protons, H-4 ($\Delta\delta_{H-4}$ = +0.77), H-6′ ($\Delta\delta_{H-6'}$ = +0.32) and H-8′ ($\Delta\delta_{H-8'}$ = +0.12), which had been shifted more downfield when comparing the chemical shifts of the un-substituted hydroxycoumarin. After comparing the ^{1}H and ^{13}C NMR chemical shifts with those of the reference, compound **3** was determined to be daphnoretin (Hu et al. 2009).

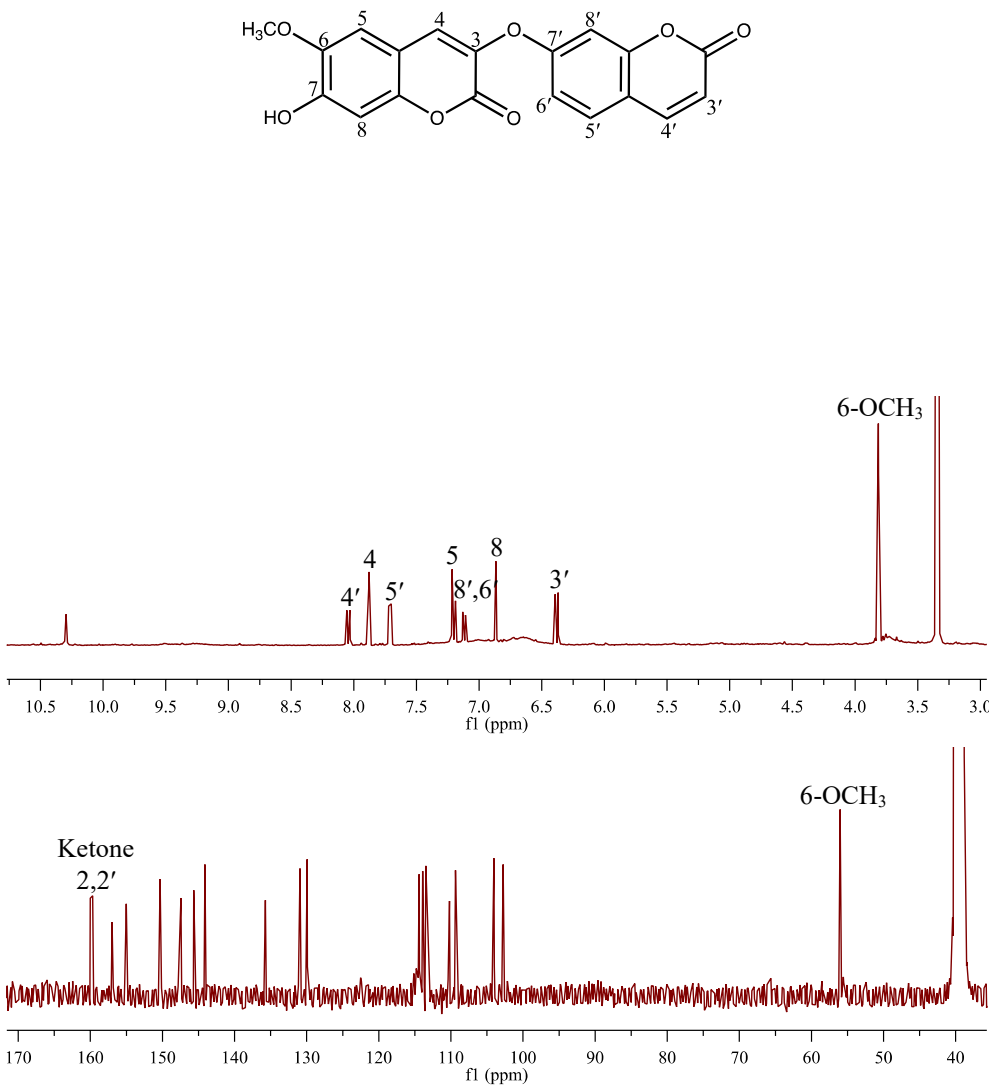

Figure 9. ^{1}H and ^{13}C NMR spectra of compound **3** in DMSO-d_6

3.1.4. Compound 4

Compound **4** was obtained as a colorless amorphous powder. The empirical formula of $C_{24}H_{20}O_{10}$ was assigned by the negative HRESIMS data of *m/z* 467.0972 $[M-H]^-$ (calcd for $C_{24}H_{19}O_{10}$, 467.0978). The UV spectrum data showed absorption maximum at 322 (3.60) and 203 (4.04) [λ_{max} (log ε)] nm. The ^{1}H-NMR spectrum of compound **4** showed four pairs of ortho coupled protons [δ_H 6.32 (1H, d, *J* = 9.6 Hz, H-3′)/8.08 (1H, d, *J* = 9.5 Hz, H-4′), 7.77 (1H, d, *J* = 8.7 Hz, H-5′)/7.30 (1H, d, *J* = 8.8 Hz, H-6′), 6.18 (1H, d, *J* = 9.4 Hz, H-3)/8.01 (1H, d, *J* = 9.4 Hz, H-4), and 7.61 (1H, d, *J* = 8.6 Hz, H-5)/7.00 (1H, d, *J* = 8.6 Hz, H-6)]. These signals were assignable to two coumarin monomers that are linearly linked together. Based on the anomeric proton [δ_H 5.47 (1H, s)], a rhamnosyl unit could be deduced, and the configuration at the C-1″ anomeric rhamnosyl signal was determined to be α-configuration. The ECD spectra of compound **4** (Figure 12) showed that there was a negative Cotton effect observed at 330 nm as a result of the exiton interaction. Comparing with the reference data (Baba et al. 1990), the 8–8′ axial chirality was determined to be *P.* From the obtained signal patterns and the literature data, compound **4** was matched with edgeworoside C (Baba et al. 1990).

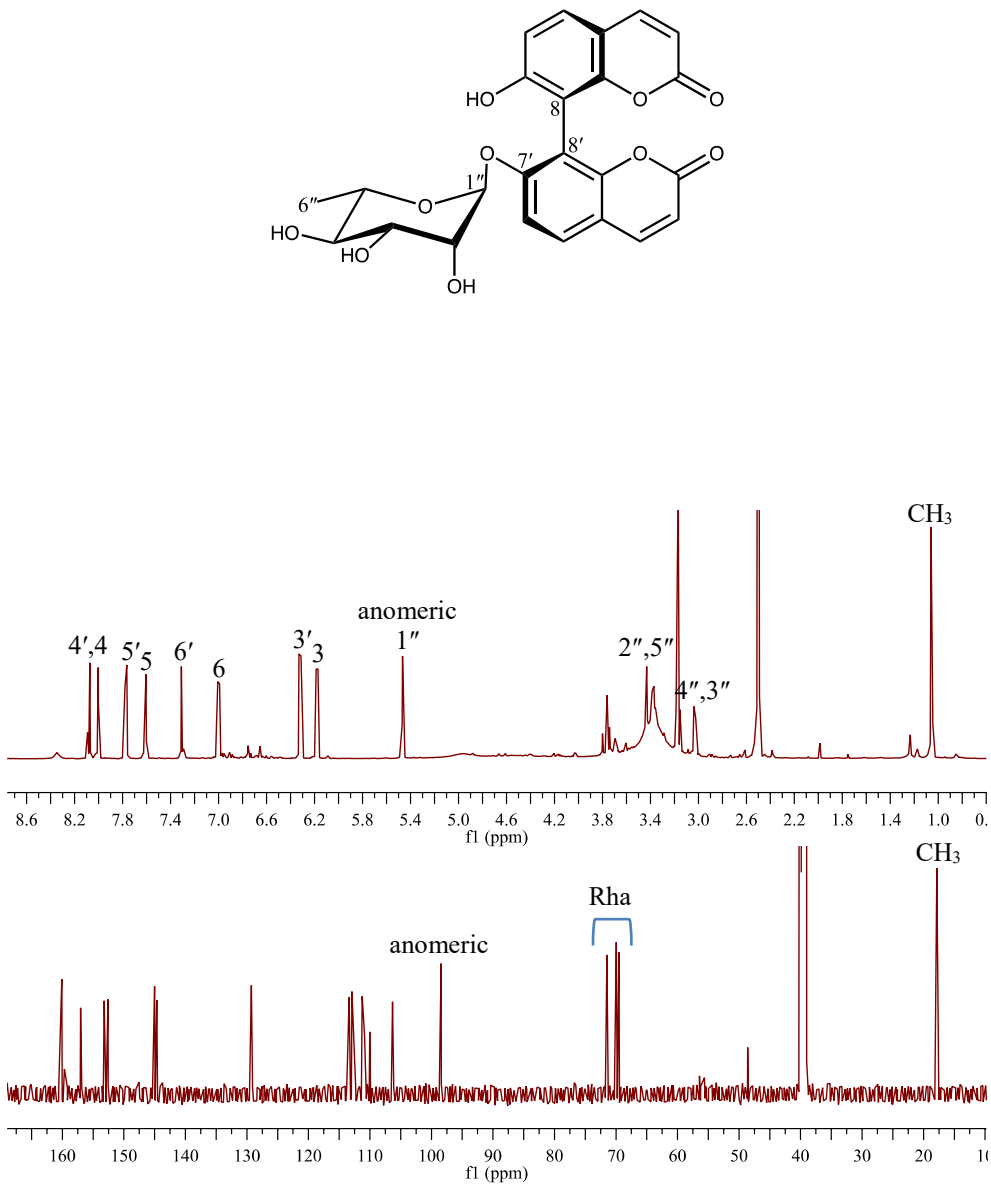

Figure 10. ^{1}H and ^{13}C NMR spectra of compound **4** in DMSO-d_6

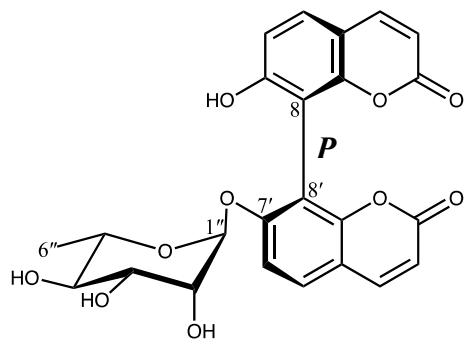

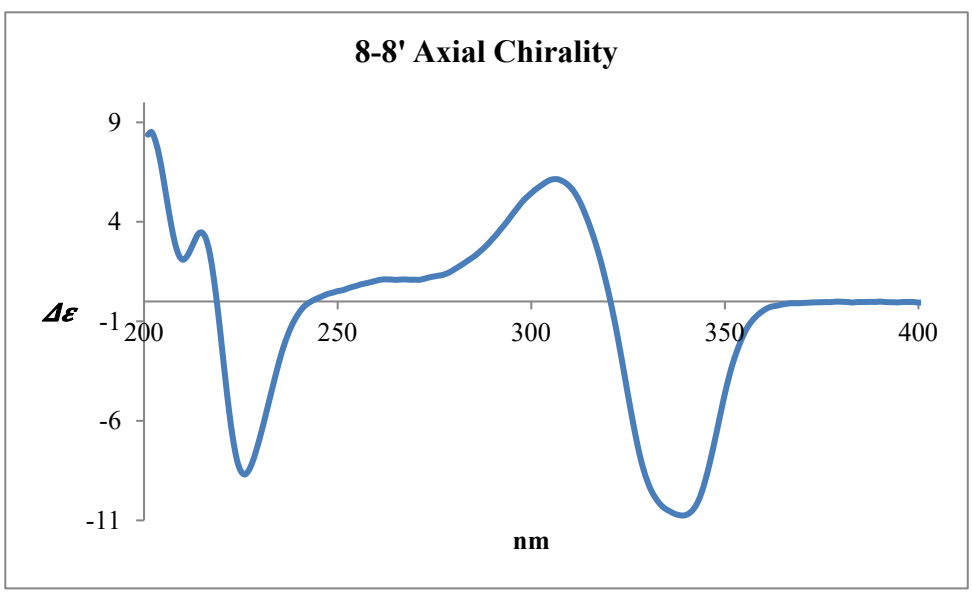

Figure 11. ECD spectrum of compound **4**

3.1.5. Compound 5

Compound **5** was isolated as a colorless crystalline powder. The negative HRESIMS data of **5** was *m/z* 613.0980 $[M-H]^-$ (calcd for $C_{32}H_{21}O_{13}$, 613.0982), corresponding to the molecular formula $C_{32}H_{22}O_{13}$. The UV spectrum data showed absorption maxima at 325 (3.49) and 207 (3.69) [λ_{max} (log ε)] nm, which are characteristics of 7-oxycoumarins.

The ^{1}H-NMR spectrum of compound **5** indicated the presence of a 7-coumarinyloxy group [δ_H 6.37 (1H, d, *J* = 9.6 Hz, H-3′), 8.03 (1H, d, *J* = 9.6 Hz, H-4′), 7.68 (1H, d, *J* = 8.7 Hz, H-5′), 7.09 (1H, dd, *J* = 8.5, 2.5 Hz, H-6′) and 7.19 (1H, d, *J* = 2.5 Hz, H-8′)], a 3,7-dioxycoumarin-8-yl group [δ_H 7.97 (1H, s, H-4), 7.60 (1H, d, *J* = 8.6 Hz, H-5) and 7.02 (1H, d, *J* = 8.5 Hz, H-6)], and a 7-oxycoumarin-8-yl group [δ_H 6.32 (1H, d, *J* = 9.3 Hz, H-3″), 8.08 (1H, d, *J* = 9.6 Hz, H-4″), 7.77 (1H, d, *J* = 8.7 Hz, H-5″) and 7.24 (1H, d, *J* = 8.7 Hz, H-6″)]. The ^{1}H NMR signals were very similar to those of edgeworoside A (Baba et al., 1989), except for the signals corresponding to an apiosyl sugar moiety instead of a rhamnosyl group. The configuration of the apiosyl group at C-1 was deduced to be β from the coupling constant (*J* = 2.4 Hz) of H-1‴ and was determined to be D-apiosyl sugar moiety by further comparison of the ^{1}H NMR and ^{13}C NMR spectral data with standard reference data (Pfeffer et al. 1979).

In addition to the ^{13}C NMR signals corresponding to the aforementioned ^{1}H NMR signals, the ^{13}C NMR spectrum showed three carbonyl signals (δ_C 160.2, 159.9 and 156.7) characteristic of a *α,β*-unsaturated lactone carbonyl carbon, seven quaternary carbon signals attached to an oxygen atom (δ_C 159.6, 159.0, 157.6, 155.0, 152.6, 151.1 and 134.9) and five quaternary carbon signals (δ_C 144.4, 113.2,

110.5, 109.9 and 106.7).

The construction of the four subunits was achieved with the aid of the HMBC experiment and literature comparison. The ether linkage between C-3 and C-7′ could be deduced based on the chemical shifts of the adjacent protons (H-4, H-6′ and H-8′), which were more deshielded ($\Delta\delta_{H\text{-}4}$ = +0.86, $\Delta\delta_{H\text{-}6'}$ = +0.29, $\Delta\delta_{H\text{-}8'}$ = +0.44) compared to hydroxyl-unsubstituted 3-hydroxycoumarin and 7-hydroxycoumarin. The attachment of the sugar moiety to the trimeric coumarin skeleton at C-7″ was determined on the basis of the key HMBC cross signals (Figure 14) between H-1‴ (δ_H 5.64) and C-7″ (δ_C 157.6). The 8–8″ axial chirality was determined to be *M,* based on the ECD spectrum (Figure 15), and comparing the positive Cotton effect observed at the exiton interaction at 330 nm with that of the literature (Baba et al. 1989). Based on the spectral data obtained and comparing them with the reference data, compound **5** was determined to be edgeworoside B (Baba et al. 1990).

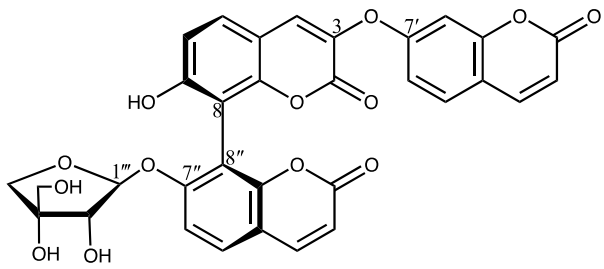

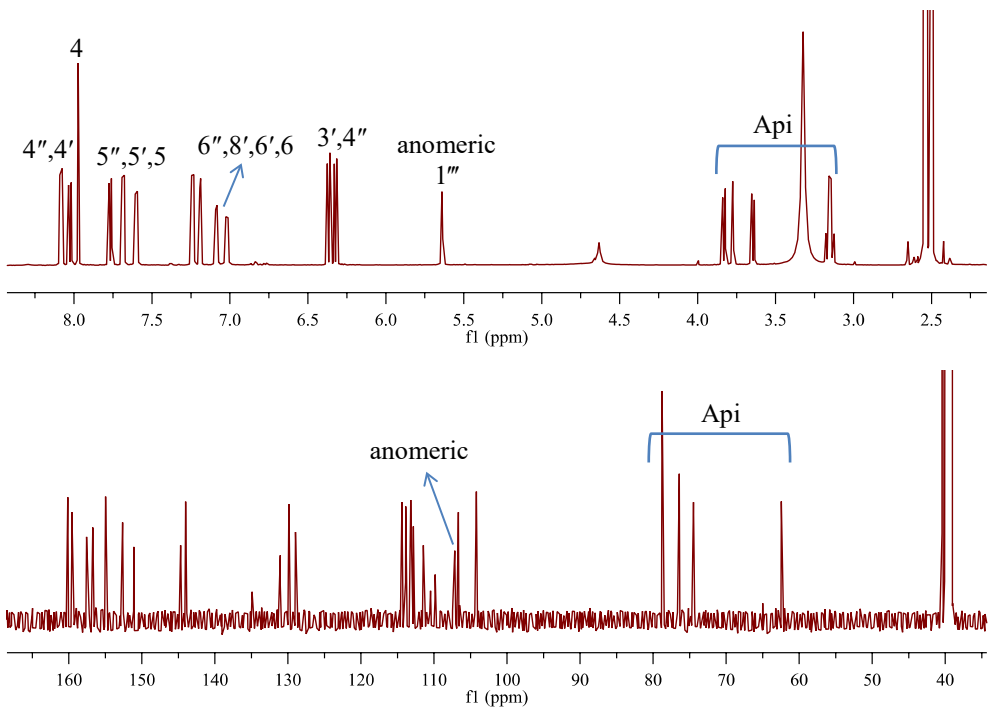

Figure 12. ^{1}H and ^{13}C NMR spectra of compound **5** in DMSO-d_6

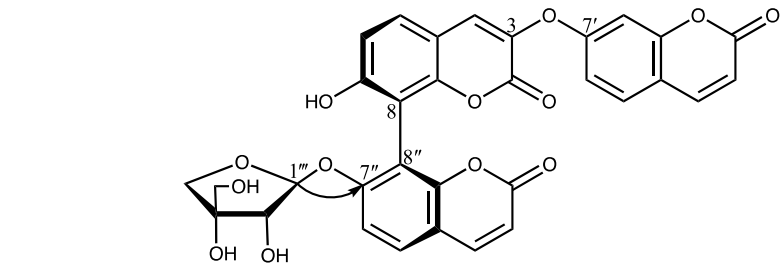

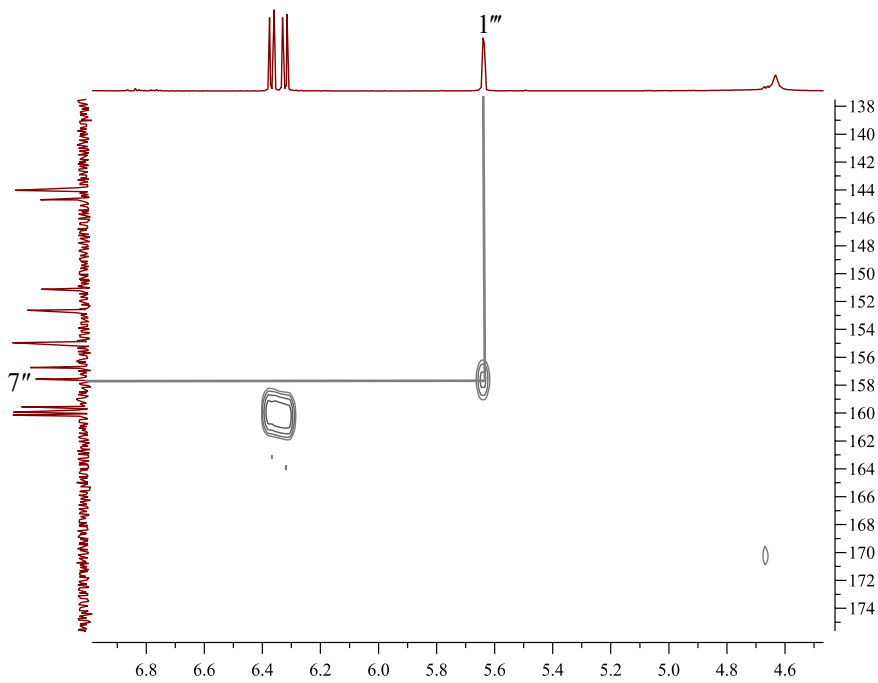

Figure 13. Key HMBC spectrum of compound **5**

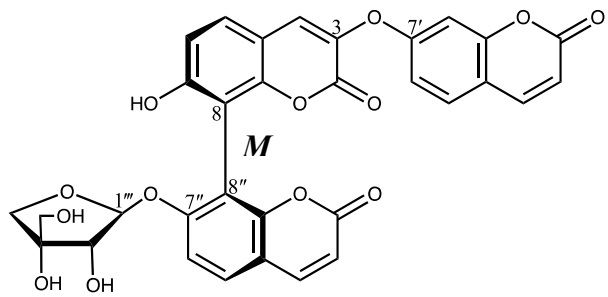

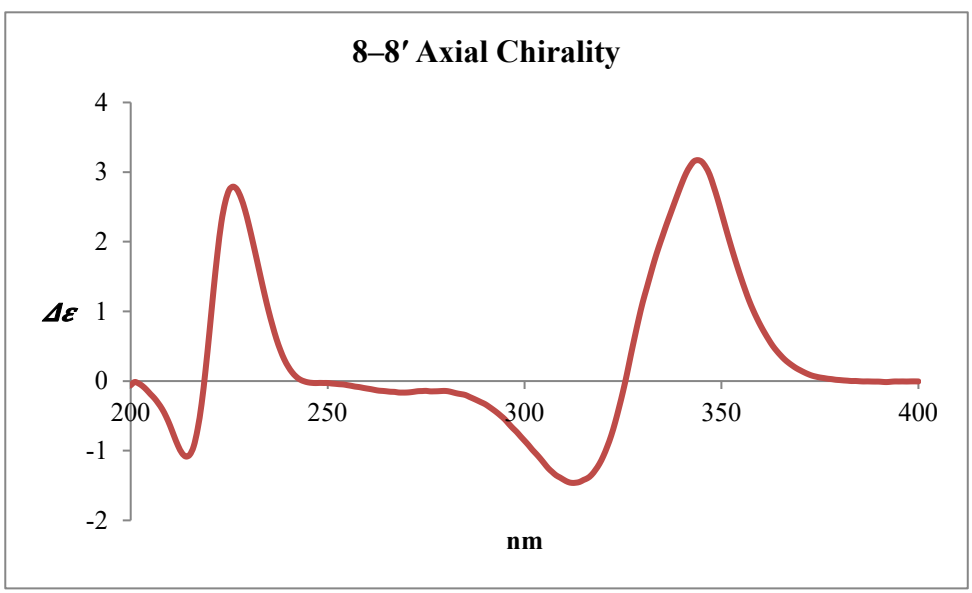

Figure 14. ECD spectrum of compound **5**

3.1.6. Compound 6

Compound **6** was isolated as a pale yellow amorphous powder. The negative HRESIMS data of **6** was *m/z* 643.1085 $[M-H]^-$ (calcd for $C_{33}H_{23}O_{14}$, 643.1088), leading to the molecular formula of $C_{33}H_{24}O_{14}$. The UV spectrum exhibited absorption maxima at 325 (3.59) and 200 (4.09) [λ_{max} (log ε)] nm, from which the 7-oxycoumarin structure could be assumed.

The ^{1}H-NMR and ^{13}C NMR spectrum of compound **6** were very similar to those of compound **5,** in which the signals corresponding to a linearly linked coumarin trimers were identified. Namely, 7-coumarinyloxy group [δ_H 6.35 (1H, d, *J* = 9.5 Hz, H-3′), 8.02 (1H, d, *J* = 9.6 Hz, H-4′), 7.68 (1H, d, *J* = 8.6 Hz, H-5′), 7.04 (1H, dd, *J* = 8.5, 2.5 Hz, H-6′) and 7.12 (1H, d, *J* = 2.5 Hz, H-8′)], a 3,7-dioxycoumarin-8-yl group [δ_H 7.95 (1H, s, H-4), 7.50 (1H, d, *J* = 8.6 Hz, H-5) and 6.90–6.86 (1H, d, *J* = 8.5 Hz, H-6)], and a 7-oxycoumarin-8-yl group [δ_H 6.32 (1H, d, *J* = 9.5 Hz, H-3″), 8.08 (1H, d, *J* = 9.5 Hz, H-4″), 7.75 (1H, d, *J* = 8.7 Hz, H-5″) and 7.29 (1H, d, *J* = 8.7 Hz, H-6″)] were assignable to the tricoumarin skeleton. Unlike compound **5**, the glucose signals were observed with H-1‴ anomeric proton [δ_H 5.01 (1H, d, *J* = 7.7 Hz)]. The configuration of the anomeric proton was deduced to be β due to the large coupling constant.

The ether linkage between the glucosyl moiety and the coumarin skeleton was confirmed by the HMBC correlation between H-1‴ (δ_H 5.01) and C-7″ (δ_C 158.4). Similar to compound **4** and **5**, the axial chirality at C8–C8″ was determined by observing the exiton interaction occurring at 330 nm. Due to the positive Cotton effect on the ECD spectrum (Figure 18), the axial chirality was determined to be *S,* when comparing the ECD data with those of the reference (Baba et al. 1989).

Based on the obtained patterns of the spectral data and comparing the signals with the literature values, compound **6** was determined to be a known reported structure of 7''-*O*-(β-D-glucopyranosyl)-triumbelletin (Hu et al. 2009).

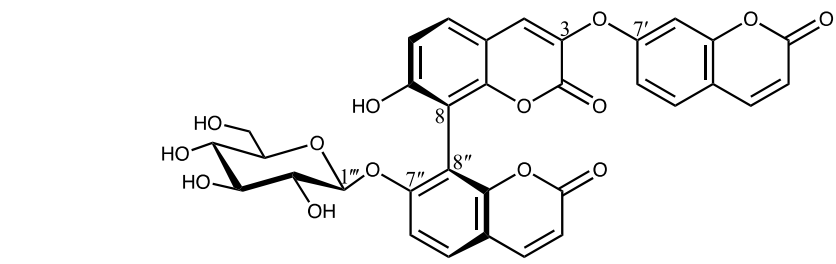

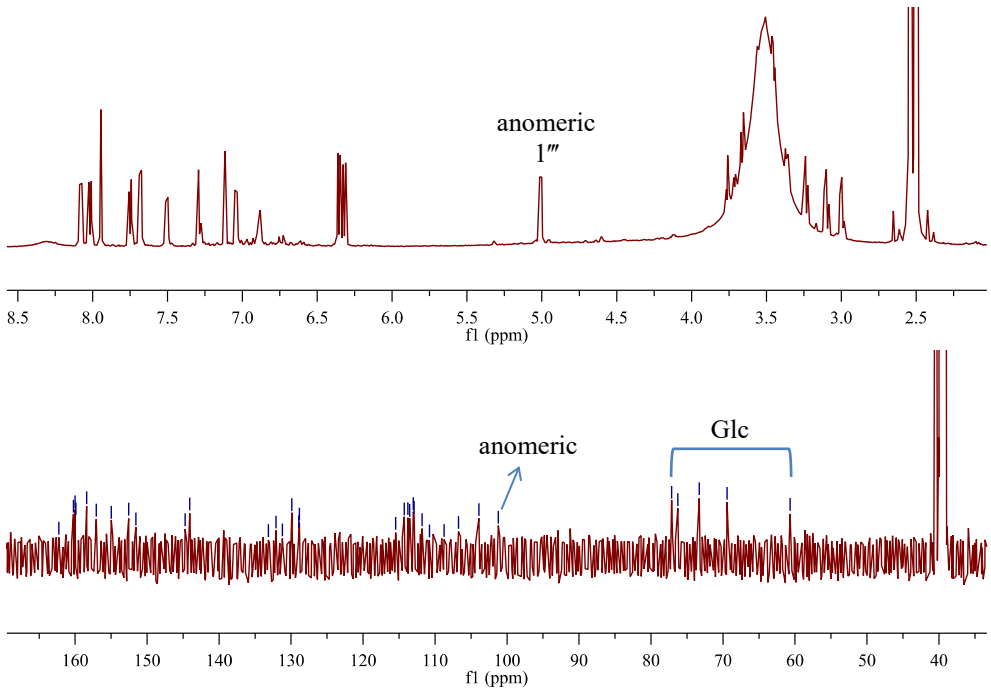

Figure 15. ^{1}H and ^{13}C NMR spectra of compound **6** in DMSO-d_6

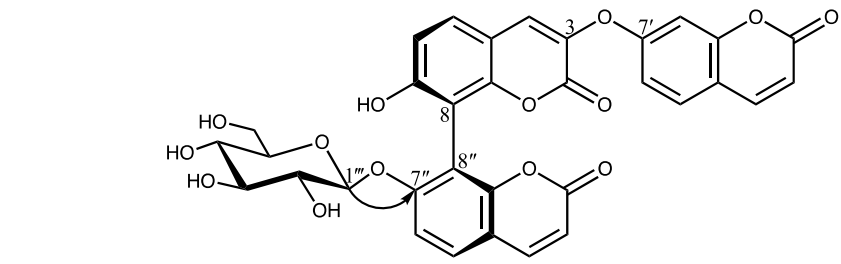

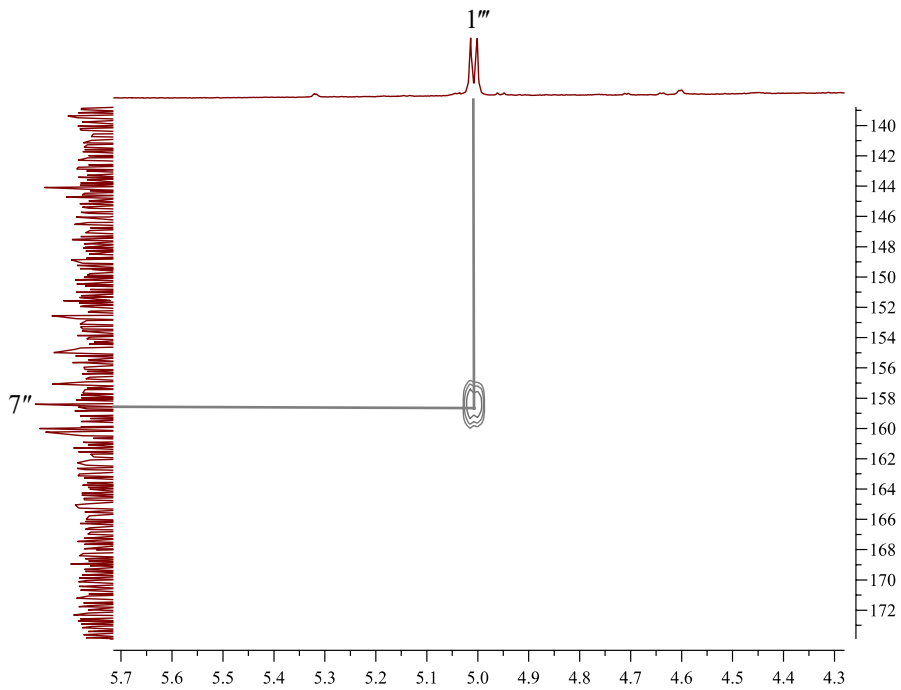

Figure 16. Key HMBC spectrum of compound **6**

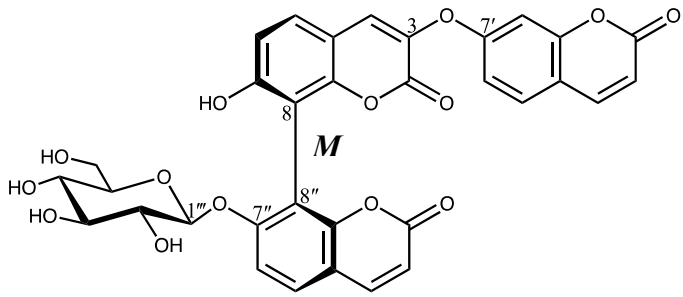

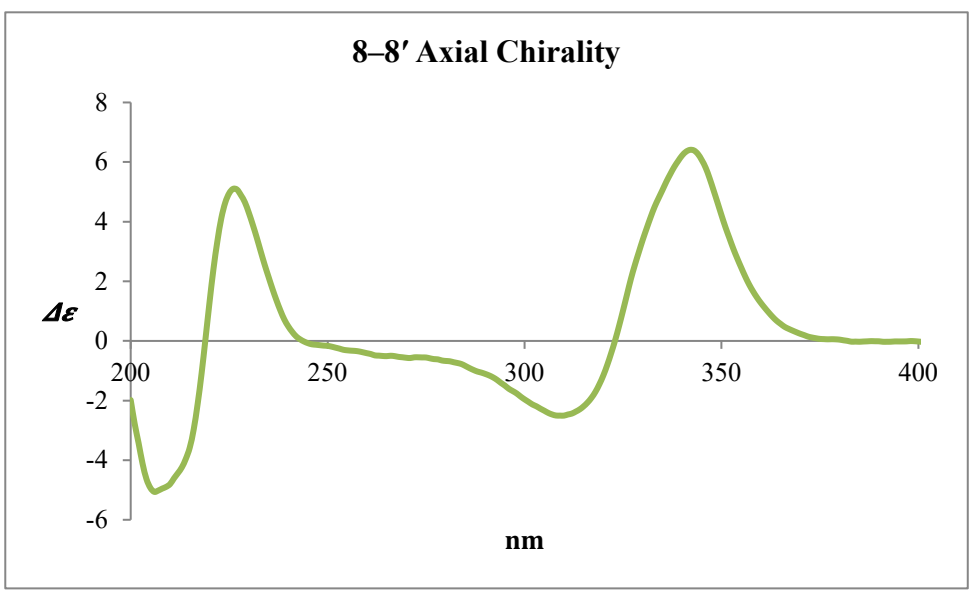

Figure 17. ECD spectrum of compound **6**

3.1.7. Compound 7

Compound **7** was obtained as a pale yellow amorphous powder. The molecular formula $C_{30}H_{22}O_{10}$ was assigned by the negative HRESIMS data for *m/z* 541.1159 $[M-H]^-$ (calcd for $C_{30}H_{21}O_{10}$, 541.1135). The UV spectrum data showed absorption maxima at 286 (2.75) and 216 (3.22) [λ_{max} (log ε)] nm.

The ^1H NMR spectrum of compound **7** exhibited signals assignable to two pairs of 4-oxyphenyl groups [δ_H 7.06 (2H, d, *J* = 8.5 Hz, H-12,16) and 6.70 (2H, d, *J* = 8.5 Hz, H-13,15), and 7.07 (2H, d, *J* = 8.5 Hz, H-12′,16′) and 6.69 (2H, d, *J* = 8.5 Hz, H-13′,15′)], a 2,4,6-trioxyphenyl groups [δ_H 5.67 (1H, s, H-7′) and 5.46 (1H, s, H-9′)], a 3-hydroxy-2,8-disubstituted 5,7-dioxy-3,4-dihydrobenzopyran [δ_H 6.11 (1H, s, H-6), 4.57 (1H, d, *J* = 7.5 Hz, H-2), 3.83 (1H, td, *J* = 6.2 Hz, H-3), 2.84 (1H, dd, *J* = 16.0, 5.0 Hz, H-4a), and δ_H 2.52 (1H, dd, *J* = 16.0, 8.5 Hz, H-4b)], and a benzylmethine [δ_H 5.60 (1H, s, H-7′)]. The ^{13}C NMR spectrum showed 30 carbon signals, including a ketone at δ_C 197.8 (C-4′), three methine carbons attached to oxygen atoms at δ_C 96.3 (C-3′), 92.8 (C-2′) and 82.2 (C-2), and a methylene carbon signal at δ_C 28.8 (C-4). The NMR data of **7** were very similar to those of genkwanol A, suggesting that they are stereoisomers (Taniguchi et al. 1996). The relative configuration at C-2 and C-3 was *trans* based on the coupling constant of H-2/H-3 [δ_H 4.57 (1H, d, *J* = 7.5 Hz, H-2)] (Czochanska et al., 1980). The absolute configuration of C-2 (*R*)/C-3 (*S*) and C-2′ (*R*)/C-3′ (*S*) were confirmed by the ECD spectrum (Figure 21) which exhibited negative splitting Cotton effects at 280 and 330 nm and comparing it with the reference data (Taniguchi et al. 1996). Based on the patterns observed from the obtained spectral data, compound **7** was determined to be daphnodorin I (Taniguchi et al. 1996).

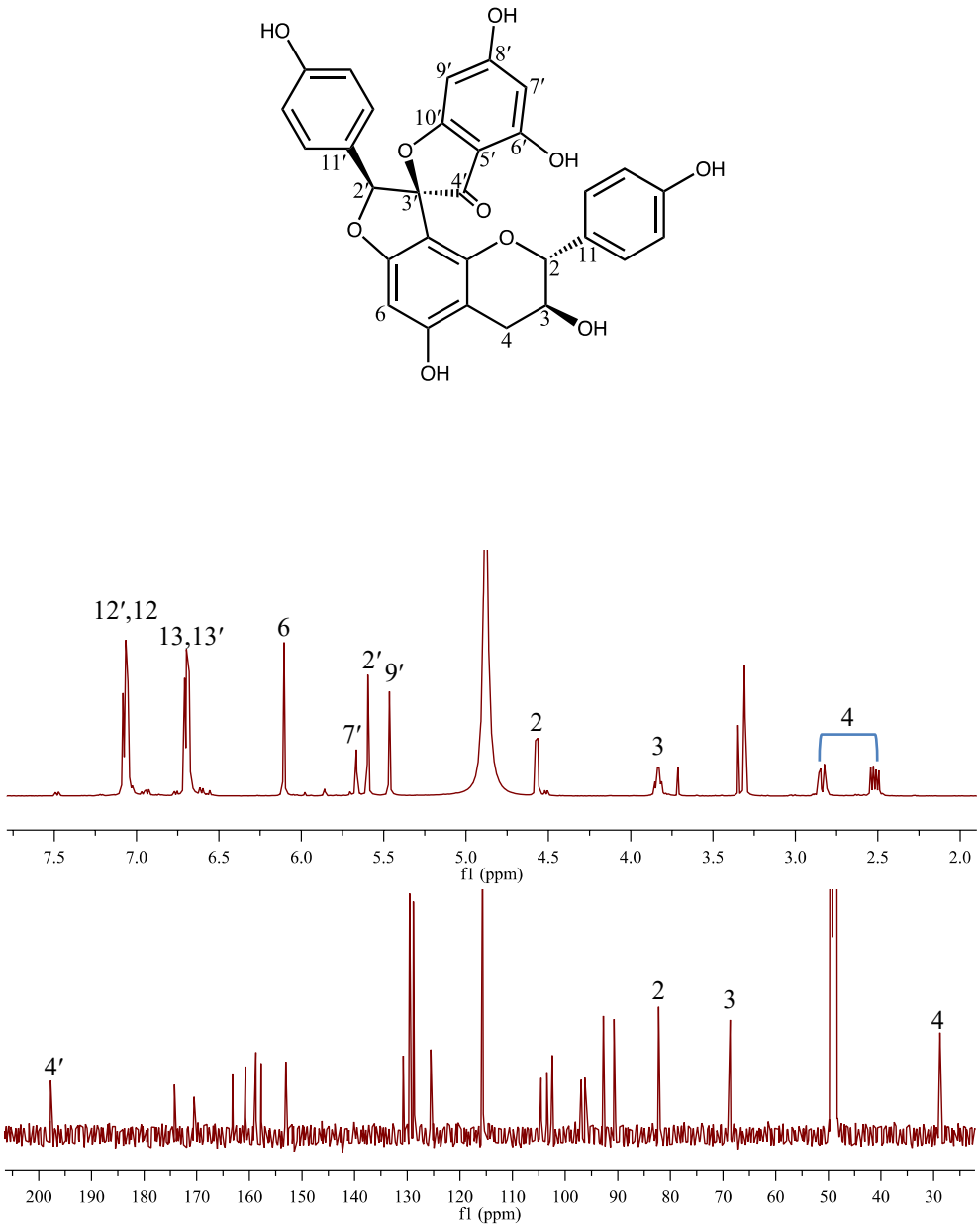

Figure 18. ^{1}H and ^{13}C NMR spectra of compound **7** in MeOD-d_4

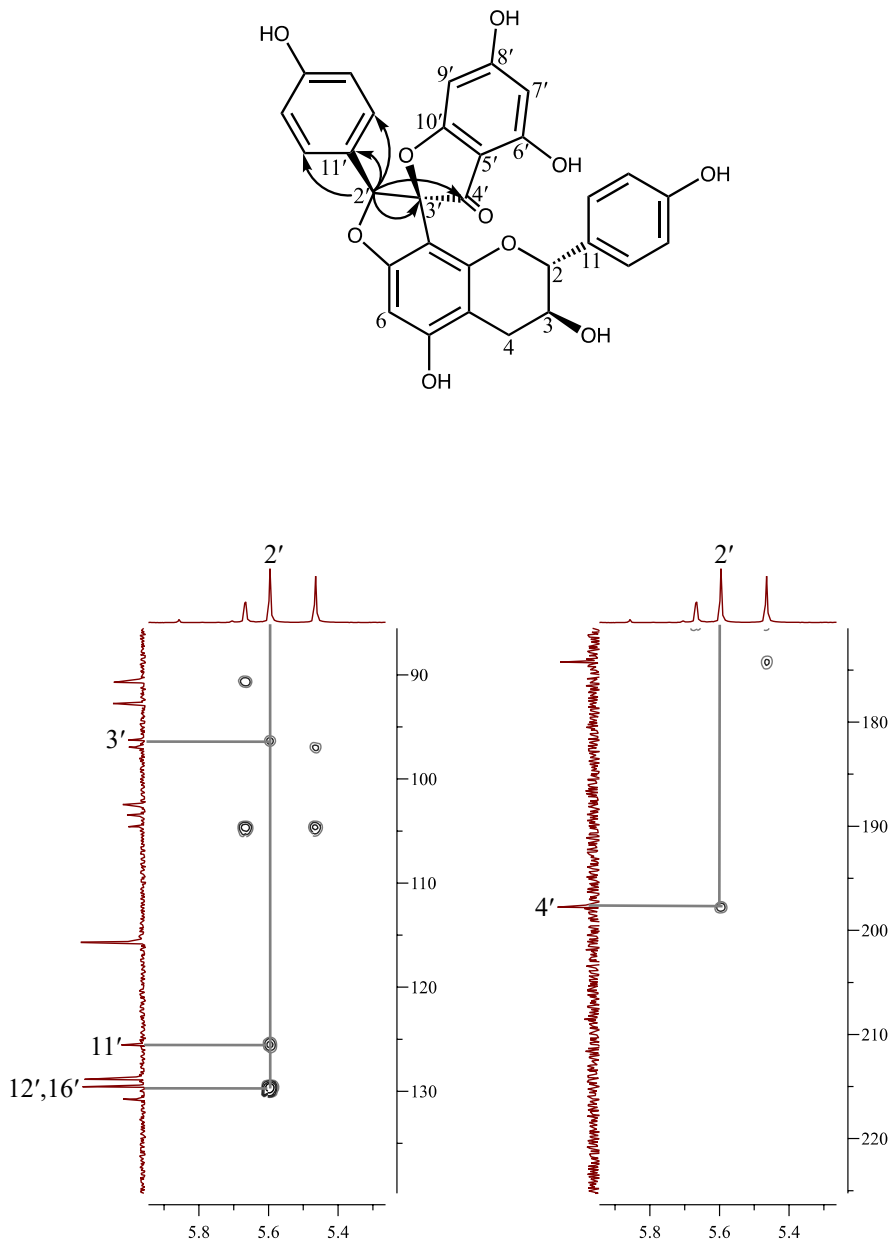

Figure 19. Key HMBC spectrum of compound **7**

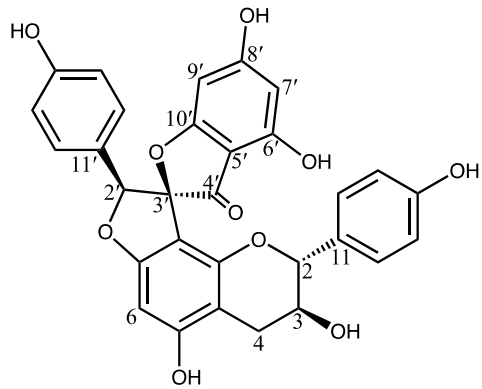

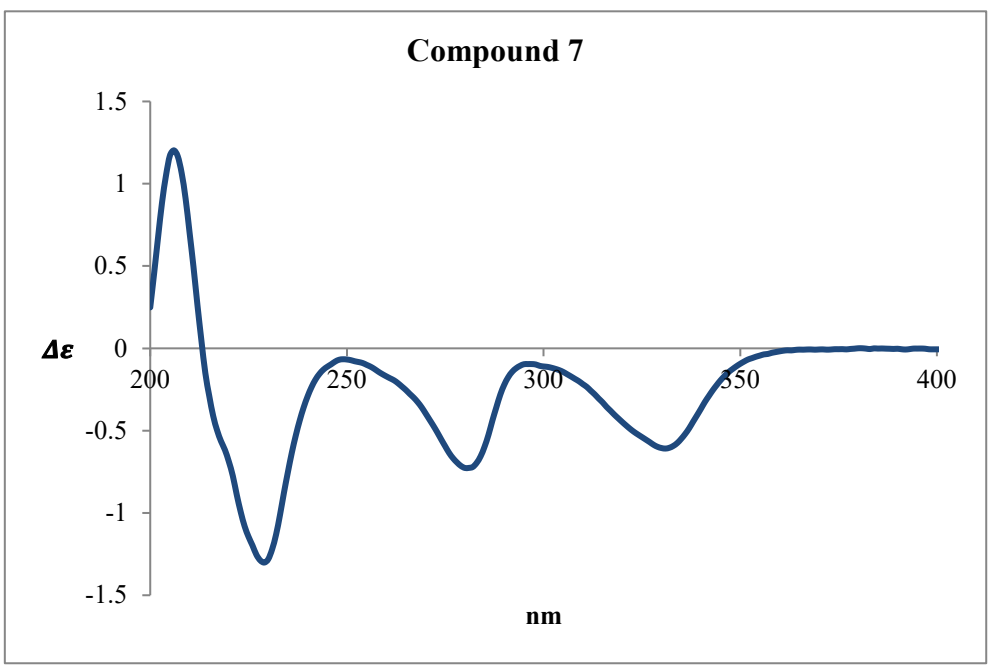

Figure 20. ECD spectrum of compound **7**

3.1.8. Compound 8

Compound **8** was isolated as a pale yellow amorphous powder. The negative HRESIMS data of **8** was m/z 541.1157 $[M-H]^-$ (calcd for $C_{30}H_{21}O_{10}$, 542.1135), corresponding to the molecular formula $C_{30}H_{22}O_{10}$. The absorption maxima were observed at 331 (3.38), 266 (3.71), and 207 (4.05) [λ_{max} (log ε)] nm.

In the ^{1}H-NMR spectrum, two pairs of 4-oxyphenyl signals [δ_H 6.68 (2H, d, *J* = 7.8 Hz, H-12,16)/6.56 (2H, d, *J* = 8.4 Hz, H-13,15), and 7.46 (2H, d, *J* = 9.0 Hz, H-12′,16′)/6.75 (2H, d, *J* = 9.0 Hz, H-13′,15′)] were observed. The proton signals at δ_H 4.67 (1H, d, *J* = 6.0 Hz, H-2), δ_H 3.75 (1H, q, *J* = 6.2 Hz, H-3), and 2.66 (1H, dd, *J* = 16.2, 4.8 Hz, H-4) in conjunction of the ^{13}C NMR signals at δ_C 82.6 (C-2), 68.7 (C-3), and 27.3 (C-4), corresponded to the 3,4-dihydrobenzopyran moiety. There was a characteristic carbonyl carbon resonance at δ_C 183.8, indicative of another flavone subunit. The ECD spectrum of compound **8** (Figure 23) showed similar splitting Cotton effect patterns as Wikstrol A (Zhang et al. 2011); therefore, the 3′–8 axial chirality was determined to be *P*. Comparing the reference data with the spectroscopic observations, compound **8** was determined to be Wikstrol A (Baba et a. 1994).

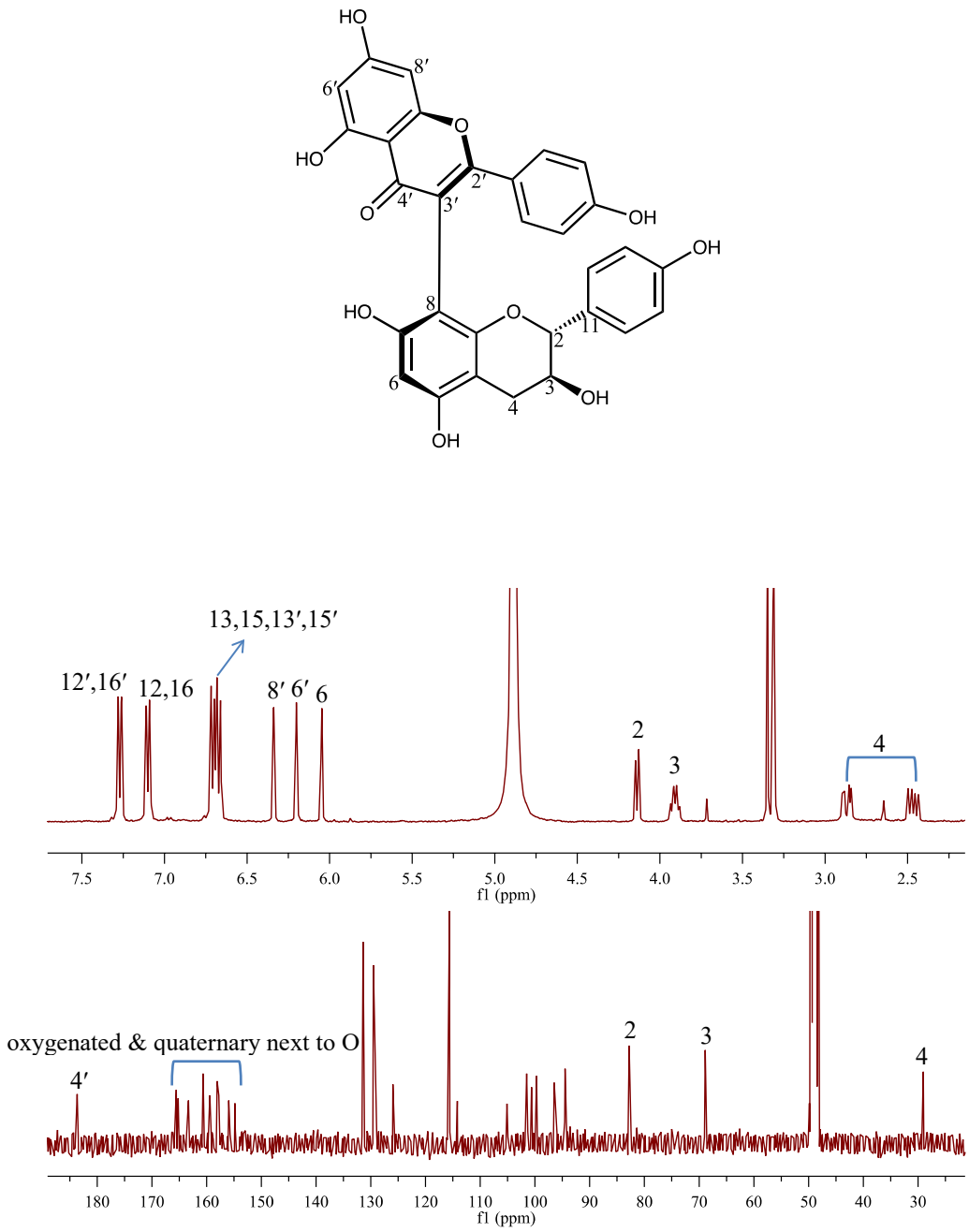

Figure 21. ^{1}H and ^{13}C NMR spectra of compound **8** in MeOD-d_4

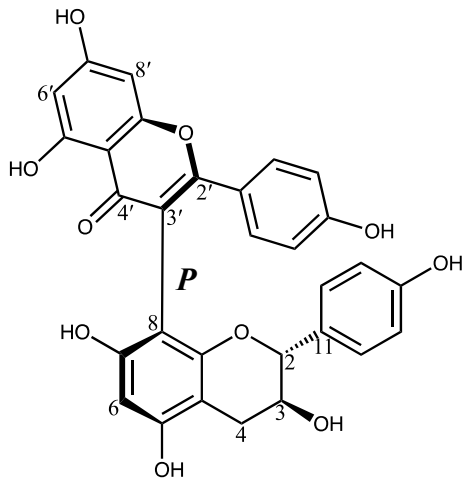

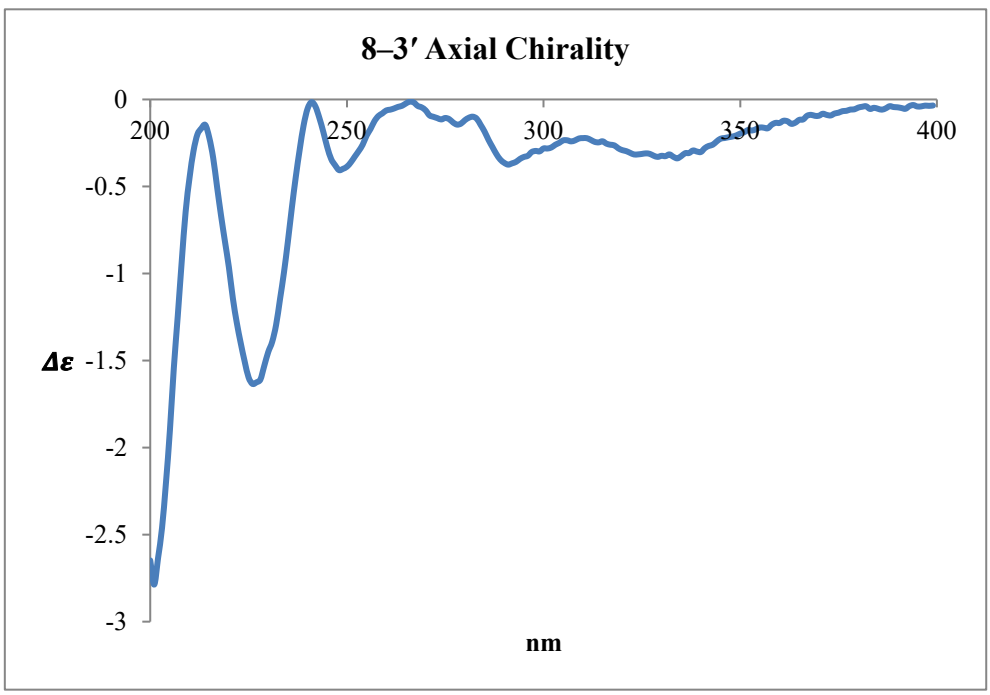

Figure 22. ECD spectrum of compound **8**

3.1.9. Compound 9

Compound **9** was isolated as a pale yellow amorphous powder. The negative HRESIMS data of **9** was m/z 541.1135 $[M-H]^-$ (calcd for $C_{30}H_{21}O_{10}$, 542.1135), corresponding to the molecular formula $C_{30}H_{22}O_{10}$. The absorption maxima were observed at 333 (3.05), 266 (3.32), and 210 (3.65) [λ_{max} (log ε)] nm.

The patterns of signals observed in the ^{1}H-NMR spectrum were very similar to those shown for compound **8**, suggesting that they are stereoisomers. First, the presence of two pairs of 4-oxyphenyl signals [δ_H 7.10 (2H, d, *J* = 8.9 Hz, H-12,16)/6.71 (2H, d, *J* = 8.0 Hz, H-13,15), and 7.27 (2H, d, *J* = 8.4 Hz, H-12′,16′)/6.67 (2H, d, *J* = 8.4 Hz, H-13′,15′)] were observed. From the proton signals at δ_H 4.14 (1H, d, *J* = 8.0 Hz, H-2), δ_H 3.94–3.88 (1H, m, H-3), and 2.87 (1H, dd, *J* = 16.0, 5.6 Hz, H-4) in conjunction of the ^{13}C NMR signals at δ_C 82.8 (C-2), 68.9 (C-3), and 29.0 (C-4), corresponded to the 3,4-dihydrobenzopyran moiety. The proton at H-2 was shifted more upfield ($\Delta\delta_{H-2}$ = -0.53) compared to compound **8** due to shielding caused by the flavone subunit. There was a characteristic carbonyl carbon resonance at δ_C 183.7. The ECD spectrum of compound **9** (Figure 23) showed similar splitting Cotton effect patterns as Wikstrol B (Zhang et al. 2011). Comparing the reference data with the observed spectral data, compound **9** was determined to be Wikstrol B (Baba et a. 1994).

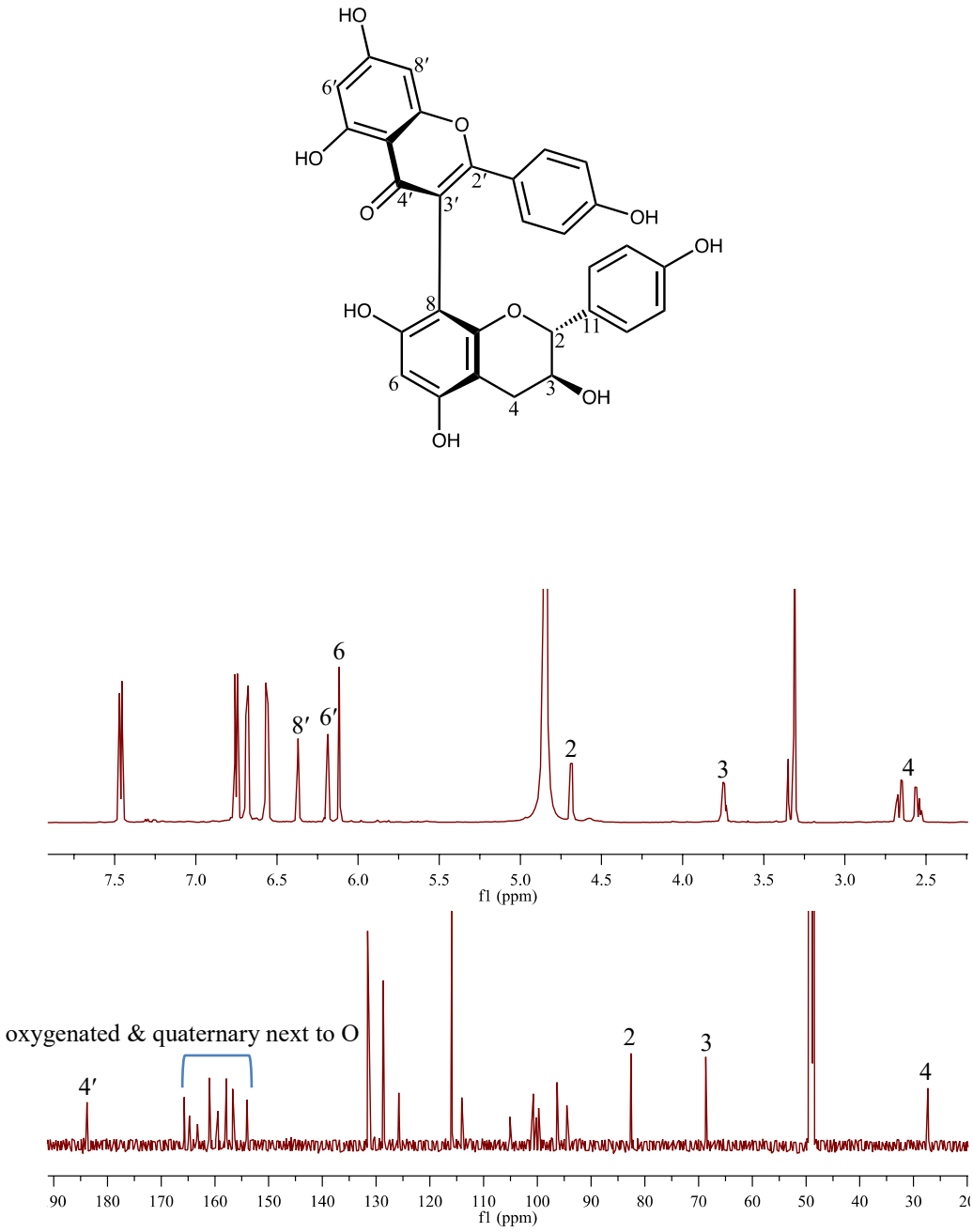

Figure 23. ^{1}H and ^{13}C NMR spectra of compound **9** in MeOD-d_4

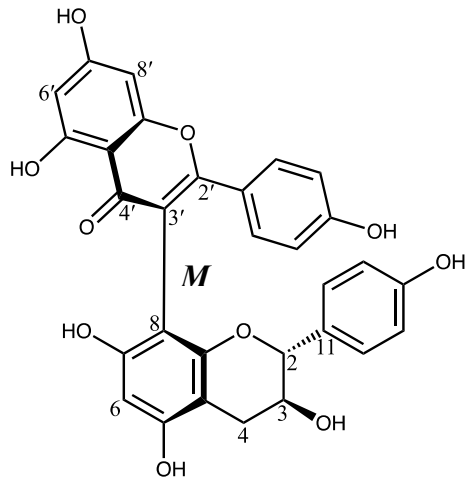

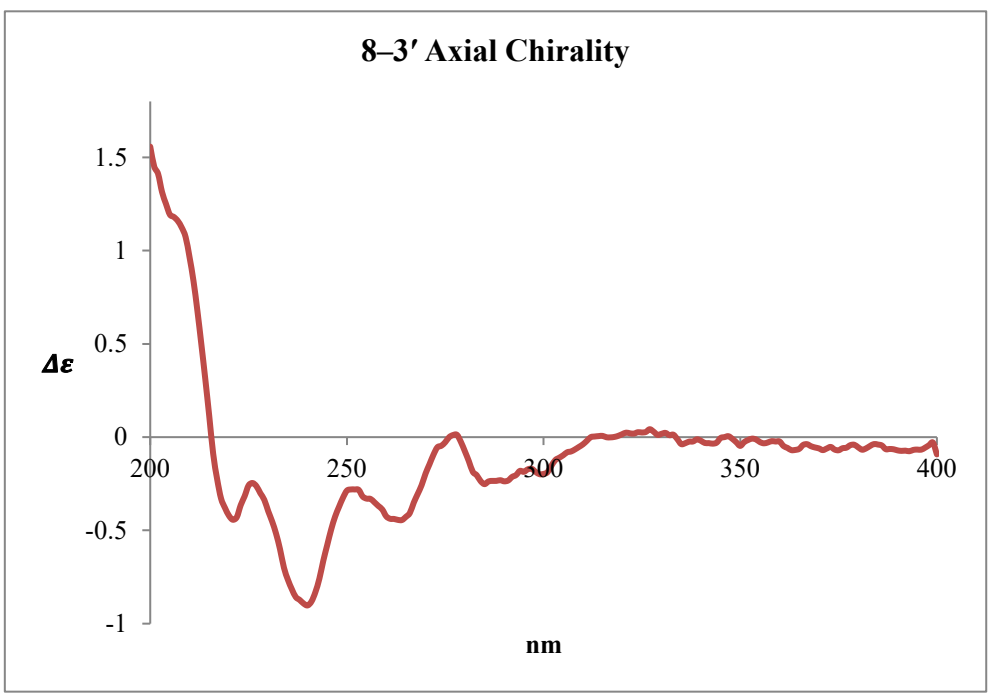

Figure 24. ECD spectrum of compound **9**

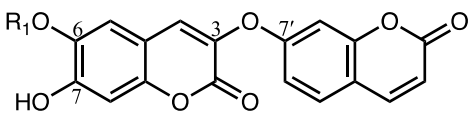

1 : R_1 = Glc
2 : R_1 = (3-hydroxy-3-methylglutarate)-Glc
3 : R_1 = CH_3

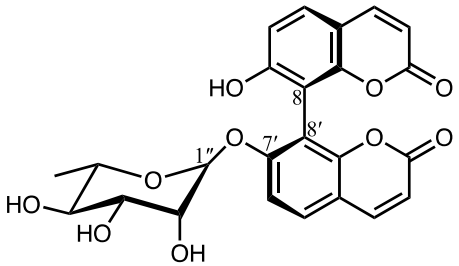

4

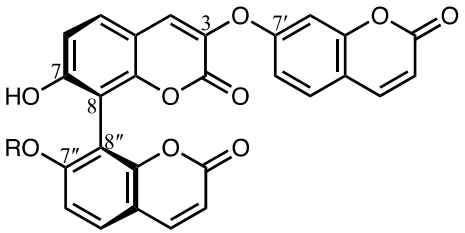

5 : R = Api
6 : R = Glc

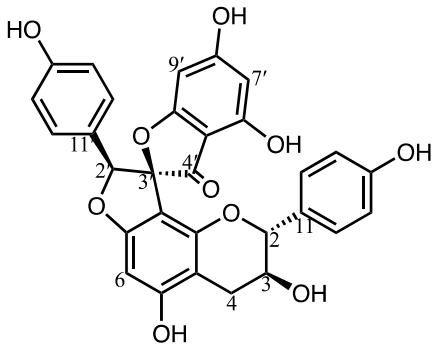

7

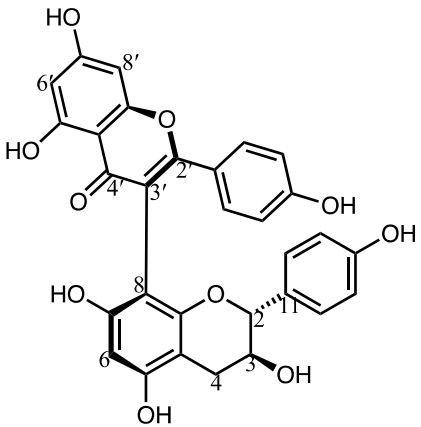

8

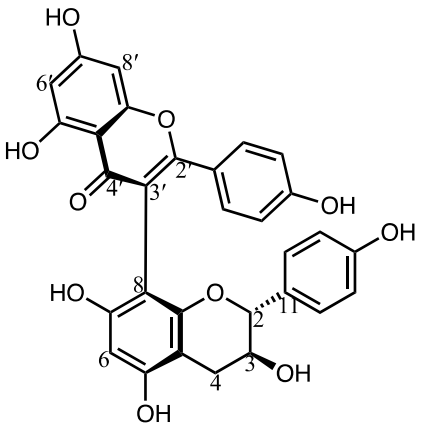

9

Figure 25. Structures of isolated compounds **1–9** from *E. chrysantha*

3.2. Bioactivity of the isolated compounds 1–9

3.2.1. Evaluation of *in vitro* cytotoxicity in 3T3-L1 adipocytes

The isolated compounds **1–9** were assessed for their *in vitro* cytotoxic effects in 3T3-L1 adipocytes. The viability levels of the cells were determined by the MTT colorimetric assay. After preincubation, the cells were exposed to the isolated compounds **1–9** at a concentration of 20 μM. The formazan quantity was measured using a microplate reader spectrophotometer at the 550 nm absorbance wavelength. The results indicated that compounds **1–9** exhibited no significant decrease in cell viability at 20 μM (Figure 24).

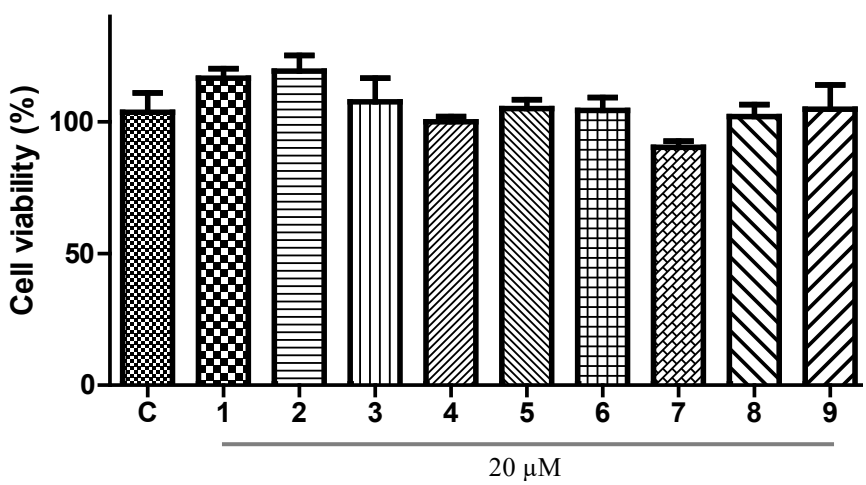

Figure 26. Effects of isolated compounds on cytotoxicity in 3T3-L1 adipocytes. The cells and test compounds at 20 μM were incubated for 24 hours. The percentages of cell viability were evaluated using the MTT colorimetric assay.

3.2.2. Evaluation of 2-NBDG uptake in 3T3-L1 adipocytes

A glucose uptake assay was conducted using 2-[N-(7- nitrobenz-2-oxa-1,3-diazol-4-yl)amino]-2-deoxy-D-glucose (2-NBDG). 2-NBDG is a fluorescent D-glucose derivative used for *in vitro* measurement of glucose uptake in 3T3-L1 adipocytes. In this study, isolated compounds **1–9** were assessed for their glucose uptake activity. After treating the tested compounds at a concentration of 20 μM, the amount of fluorescence was measured by a fluorescence microplate reader. The results showed that compound **1** most effectively increased 2-NBDG uptake into 3T3-L1 adipocytes.

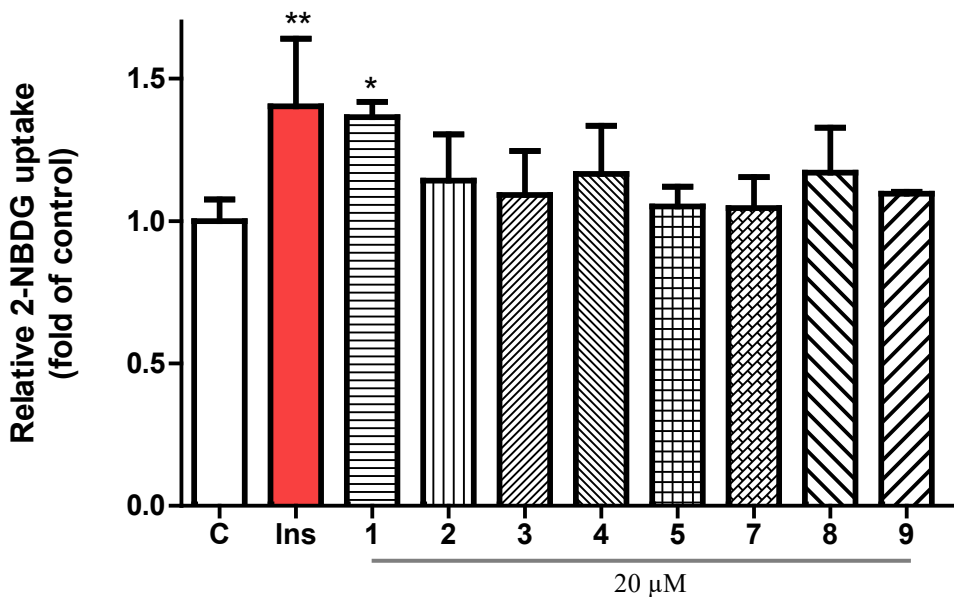

Figure 27. Evaluation of glucose uptake by insulin as positive control and compounds 1–9 in 3T3-L1 adipocytes by a fluorescent glucose probe 2-NBDG. Insulin and the isolated compounds were treated at 100 nM and 20 μM, respectively. The intensity of fluorescence was measured at ex/em = 450/535 nm. (*) $p < 0.05$, (**) $p < 0.01$, compared to the control.

IV. Conclusion

Nine compounds, including four dicoumarins (**1–4**), two tricoumarins (**5–6**), and three biflavonoids (**7–9**) were isolated from the roots of *Edgeworthia chrysantha* Lindl. Various chromatographic methods were used for separation and isolation of compounds. The structures of isolated compounds were determined by spectrometric and spectroscopic methods. Among them, 6″-*O*-(3-hydroxy-3-methylglutaryl)-daphneretusin A (**1**) was reported for the first time from nature. Additional eight known compounds, daphneretusin A (**2**), daphnoretin (**3**), edgeworoside C (**4**), edgeworoside B (**5**), 7"-*O*-(β-D-glucopyranosyl)-triumbelletin (**6**), daphnodorin I (**7**), wikstrol A (**8**), and Wikstrol B (**9**), were isolated. Among the known compounds, compounds **2–3** and **6–9** have not yet been reported from *E. chrysantha.* The isolated compounds were tested for their *in vitro* cytotoxic effects in 3T3-L1 adipocytes and exhibited no significant decrease in cell viability at 20 μM. Finally, the isolated compounds were assessed for their 2-NBDG uptake in 3T3-L1 cells. The results showed that compound **1** most effectively increased glucose uptake into adipocytes.

V. References

American Diabetes Association. (2010) Diagnosis and classification of diabetes mellitus. *Diabetes Care.* 33 (1), S62–S69.

Baba, K., Taniguti, M. & Kozawa, M. (1994) Three biflavonoids from Wikstroemia sikokiana. *Phytochemistry*. 37, 879–883.

Baba, K., Taniguti, M., Yoneda, Y. & Kozawa, M. (1990) Coumarin glycosides from *Edgeworthia chrysantha*. *Phytochemistry*. 29 (1), 247–249.

Baba, K., Tabata, Y., Taniguti, M. & Kozawa, M. (1989) Coumarins from *Edgeworthia chrysantha*. *Phytochemistry.* 28 (1), 221–225.

Chakrabarti, R., Das, B. & Banerji. (1986) Bis-coumarins from *Edgeworthia gardneri*. *Phytochemistry.* 25 (2), 557–558.

Clennett, C., Harvey, Y. & Pearman, G. (2002) Plate 433. *Edgeworthia chrysantha*. *Royal Botanic Gardens, Kew.* 19-27.

Czochanska, Z., Foo, L.Y., Newman, R.H., Porter, L. (1980) Polymeric proanthocyanidins. Stereochemistry, structural units, and molecular weight. *J. Chem. Soc*. 1, 2278–2286.

Dewick, P.M. (2009) Medicinal Natural Products: A Biosynthetic Approach, 3rd

Edition. *John Wiley & Sons, Ltd.*

eFloras. (2008) Published on the Internet http://www.efloras.org [accessed 10 December 2019] Missouri Botanical Garden, St. Louis, MO & Harvard University Herbaria, Cambridge, MA.

Gao, D., Zhang, Y. I., Yang, F. Q., Li, F., Zhang, Q. H. & Xia, Z. N. (2016) The flower of *Edgeworthia gardneri* (wall.) Meisn. suppresses adipogenesis through modulation of the AMPK pathway in 3T3-L1 adipocytes. *J Ethnopharmacol*. 191, 379–386.

Gravel, E. & Poupon, E. (2008) Biogenesis and biomimetic chemistry: can complex natural products be assembled spontaneously? *Eur J Org Chem*. 1, 27–42.

Geiger, H. & Quinn, C. (1988) Biflavonoids. *The Flavonoids, Advances in Research Since 1980*. Harborne, J. B., Ed., Chapman & Hall, New York, 21.

Gontijo, V.S., Dos Santos, M.H. & Viegas, C. Jr. (2017) Biological and chemical aspects of natural biflavonoids from plants: a brief review. *Mini-Rev Med Chem.* 17 (10), 834–862.

Hattori, Y., Horikawa, K.H., Makabe, H., Hirai, N., Hirota, M. & Kamo, T. (2007) A refined method for determining the absolute configuration of the 3-hydroxy-3-methylglutaryl group. *Tetrahedron*: *Asymmetry.* 18, 1183–1186.

Hashimoto, T., Tori, M. & Asakawa, Y. (1991) Piscicidal sterol acylglucosides from *Edgeworthia chrysantha*. *Phytochemistry*. 30 (9), 2927–2931.

Hu, X. J., Jin, H. Z., Zhang, W. D., Zhang, W., Yan, S. K., Liu, R. H., Shen, Y. H. & Xu, W. Z. (2009) Two new coumarins from *Edgeworthia chrysantha*. *Nat Prod Res*. 23 (13), 1259–1264.

Hu, X. J., Jin, H., Zhang, W., Yan, S. Xu, W., Liu, R. H., Shen, Y. & Zhang, W. D. (2009) Chemical constituents of *Edgeworthia chrysantha*. *Chem Nat Compd*. 45 (1), 126–128.

Hu, Z. J., Jin, H. Z., Xu, W. Z., Chen, M., Liu, X. H., Zhang, W., Su, J., Zhang, C. & Zhang, W. D. (2008) Anti-inflammatory and analgesic activities of *Edgeworthia chrysantha* and its effective chemical constituents. *Biol Pharm Bull*. 31 (9), 1761–1765.

Hughes, S. (1978) Washi: the world of Japanese paper. Kodansha International, Tokyo.

Kim, H.P., Park, H., Son, K.H., Chang, H.W. & Kang, S.S. (2008) Biochemical pharmacology of biflavonoids: implications for anti-inflammatory action. *Arch Pharm Res*. 31 (3), 265–273.

Kooti, W., Farokhipour, M., Asadzadeh, Z., Ashtary-Larky, D. & Asadi-Samani, M. (2016) The role of medicinal plants in the treatment of diabetes: a systematic

review. *Electron Physician*. 8 (1), 1832–1842.

Kreher, B., Neszmélyi, A. & Wagner, H. (1990). Triumbellin, a tricoumarin rhamnopyranoside from Daphne mezereum. *Phytochemistry*. 29 (11), 3633–3637.

Lake, B.G. (1999) Coumarin metabolism, toxicity and carcinogenicity: relevance for human risk assessment. *Food Chem Toxicol*. 37, 423–253.

Levien, T. L. & Baker, D. E. B. (2009) New drugs in development for the treatment of diabetes. *Diabetes Spectrum.* 22 (2), 92–106.

Li, X. N., Tong, S. Q., Cheng, D. P., Li, Q. Y. & Yan J. Z. (2014) Coumarins from *Edgeworthia chrysantha. Molecules*. 19, 2042–2048.

Li, S. S., Gao, Z., Feng, X. & Hecht, S. M. (2004) Biscoumarin derivatives from *Edgeworthia gardneri* that inhibit the lyase activity of DNA polymerase β. *J Nat Prod.* 67, 1608–1610.

Ma, Y. Y., Zhao, D. G., Zhou, A. Y., Zhang, Y. Du, Z. & Zhang, K. (2015) α-Glucosidase inhibition and antihyperglycemic activity of phenolics from the flowers of *Edgeworthia gardneri*. *J Agric Food Chem*. 63, 8162–8169.

Majumder, P. L., Sengupta, G. C., Dinda, B. N. & Chatterjef, A. (1974) Edgeworthin, a new bis-coumarin from *Edgeworthia gardneri. Phytochemistry*. 13, 1929–1931.

Menezes, J. C. J M. D. S. & Diederich, M. F. (2019) Natural dimers of coumarin, chalcones, and resveratrol and the link between structure and pharmacology. *Eur J Med.* 182, 111637.

Pescitelli, G. (2018) For a correct application of the CD exciton chirality method: the case of laucysteinamide A. *Mar Drugs.* 16, 388.

Pfeffer, P. E., Valentine K. M. & Parrish F. W. (1979) Deuterium-induced differential isotope shift 13C NMR. 1. Resonance reassignments of mono- and disaccharides. *J Am Chem Soc*. 101 (5), 1265–1274.

Taniguchi, M., Baba, K. (1996) Three biflavonoids from *Daphne odora*. *Phytochemistry.* 42, 1447–1453

Tong, S., Yan, J., Chen, G. & Lou, J. (2009) Purification of rutin and nicotiflorin from the flowers of *Edgeworthia chrysantha* Lindl. by high-speed counter-current chromatography. *J Chromatogr Sci*. 47, 341–344.

The Plant List. (2013) Version 1.1. Available at: http://www.theplantlist.org/ (Accessed: 20 November 2019).

World Health Organization. (2016) Diabetes. Available at: https://www.who.int/health-topics/diabetes (Accessed: 06 December 2019).

Xu, P., Xia, Z. & Lin, Y. (2012) Chemical constituents from *Edgeworthia gardneri*

(Thymelaeaceae). *Biochem Syst Ecol*. 45, 148–150.

Zhang, X., Wang, G., Huang, W., Ye, W. & Li, Y. (2011) Biflavonoids from the roots of *Wikstroemia indica*. *Nat Prod Commun*. 1111–1114.

Zhang, H.J., Zhao, Y.Y. & Ouyang L. (1997) Studies on the chemical constituents from the flowers of *Edgeworthia chrysantha*. *Nat Prod Res Dev*. 9, 24–27.

Zhou, D. G., Zhou, A. Y., Du, Z., Zhang, Y., Zhang, K. & Ma, Y. Y. (2015) Coumarins with α-glucosidase and α-amylase inhibitory activities from the flower of *Edgeworthia gardneri*. *Fitoterapia*. 107, 122–127.

Zhou, T., Zhang, S. W., Liu, S. S., Cong, H. J. & Xuan, L. J. (2010) Daphnodorin dimers from *Edgeworthia chrysantha* with α-glucosidase inhibitory activity. *Phytochem Lett*, 3, 242-247.

Zhuang, M., Qiu, H., Li, P., Hu, L., Wang, Y. & Rao, L. (2018) Islet protection and amelioration of type 2 diabetes mellitus by treatment with quercetin from the flowers of *Edgeworthia gardneri*. *Drug Des Devel Ther*. 12, 955–966.

국문초록

삼지닥나무 (*Edgeworthia chrysantha* (Lindl.)) 는 팥꽃나무과 (Thymelaeaceae)에 속하는 낙엽성의 관목으로 중국, 일본 및 우리나라의 남부지방에 분포하고 있다. 예로부터 이 식물의 나무껍질은 일본에서 종이의 원료로 사용되었고 뿌리와 줄기는 전통적으로 중의학에서 검염, 류머티즘의 치료를 위해 쓰여졌다. 하얀 털로 감싸진 노란색의 꽃은 항균 치료제로서 뿐만 아니라 아름다운 모양과 향기 때문에 장식용으로도 사용되었다고 전해진다. 이전에 보고된 생리활성 연구에 따르면 삼지닥나무에는 항염증, 진통, 항균 관련 성분으로 coumarin 과 flavonoid 를 포함해 다양한 oligophenolic compound 가 구성된다고 한다. 본 연구는 삼지닥나무 지하부로부터 coumarin 과 flavonoid 계열의 화학물질을 분리하고자 하였다. 또한, 분리된 화합물을 대상으로 세포독성평가 및 glucose uptake assay 를 실시하였다.

삼지닥나무 지하부의 90 % EtOH 추출물을 *n*-hexane, EtOAc, *n*-BuOH 의 순차로 분획을 하였고 EtOAc 분획물을 대상으로 다양한 크로마토그래피 기법을 통해 총 4 종의 dimeric coumarin (**1-4**), 2 종의 trimeric coumarin glycoside (**4, 5**), 3 종의 biflavonoid (**7-9**) 를 분리하였다. 분리된 화합물의 구조결정 및 동정은 각종 분광학적 분석을 통해 얻은 데이터를 종합하여 수행하였고, 화합물 1 은 β-D-glucopyranose 기와 hydroxymethylglutaric acid 기가 붙은 coumarin dimer 계열 화합물로 천연에서는 처음 분리 보고되는 물질이다. 이외에 화합물은 daphneretusin A (**2**), daphnoretin (**3**), edgeworoside C (**4**),

edgeworoside B (**5**), 7''-*O*-(β-D-glucopyranosyl)-triumbelletin (**6**), daphnodorin I (**7**), wikstrol A (**8**) 와 Wikstrol B (**9**) 으로 동정하였다.

이후 분리된 화합물이 분화된 3T3-L1 지방세포의 생존률에 미치는 영향을 평가하였고 화합물이 20 μM 일 때 세포독성이 나타나지 않았다. 또한, 분리한 화합물에 대한 glucose uptake 조절 작용을 평가하는 실험을 실시하였고 결과적으로 compound 1 이 가장 유의한 glucose uptake activity 를 가지고 있는 것을 확인하였다.

주요어: 삼지닥나무 (*Edgeworthia chrysantha*), 팥꽃나무과 (Thymelaeaceae), coumarin, biflavonoid, glucose uptake

부록

Supplementary information

List of Figures

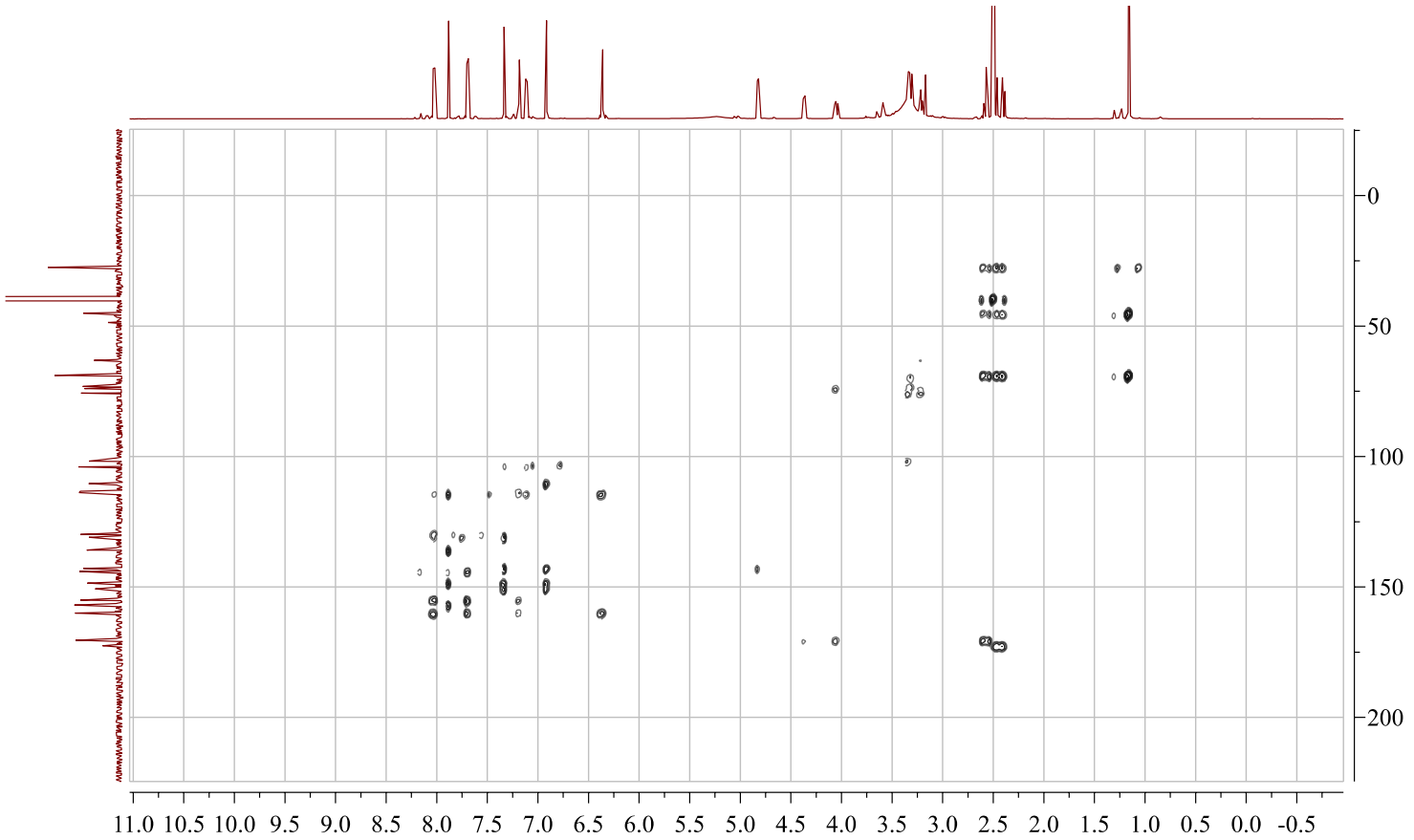

Figure S1. HMBC spectrum of compound **1** in DMSO-d_6

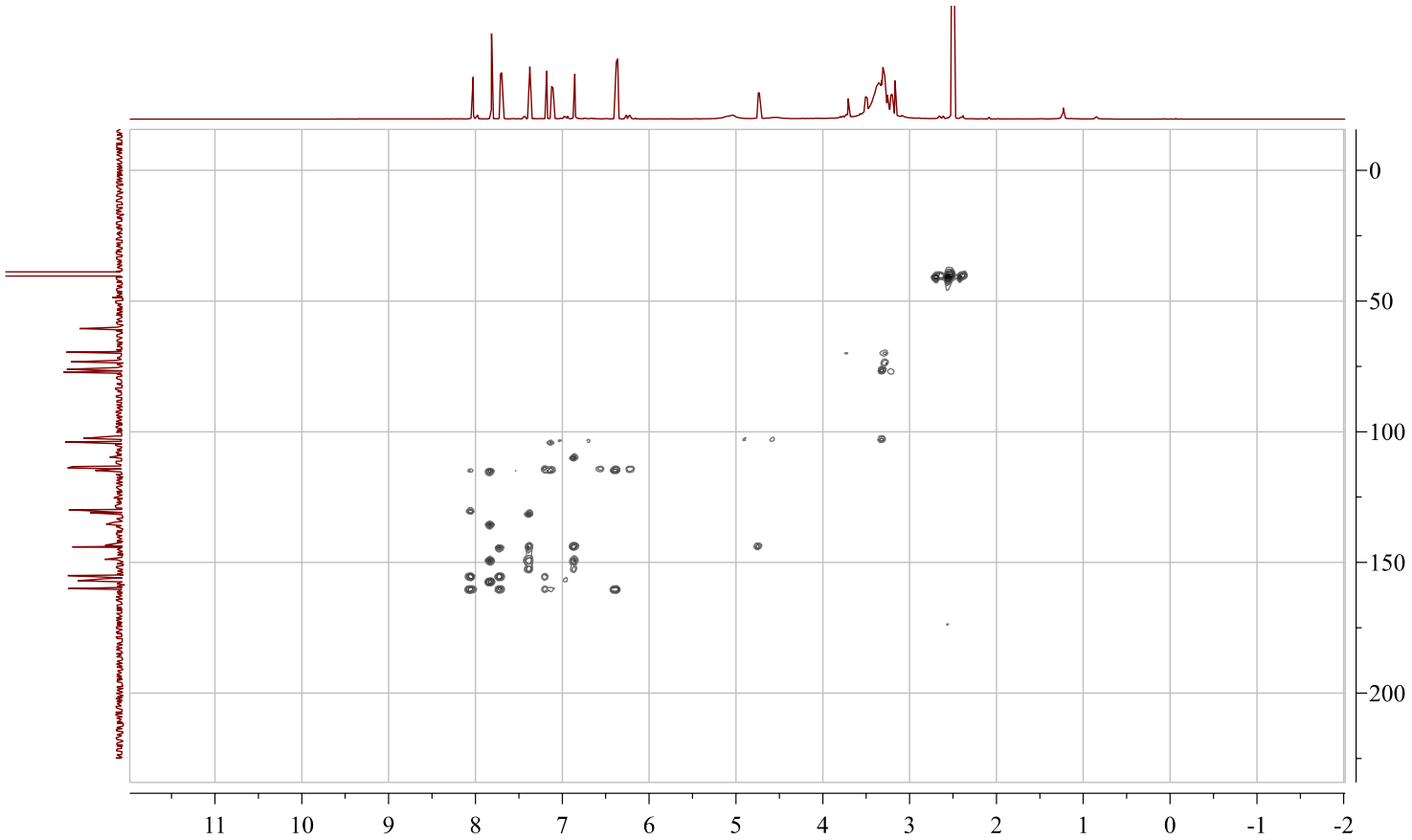

Figure S2. HMBC spectrum of compound **2** in DMSO-d_6

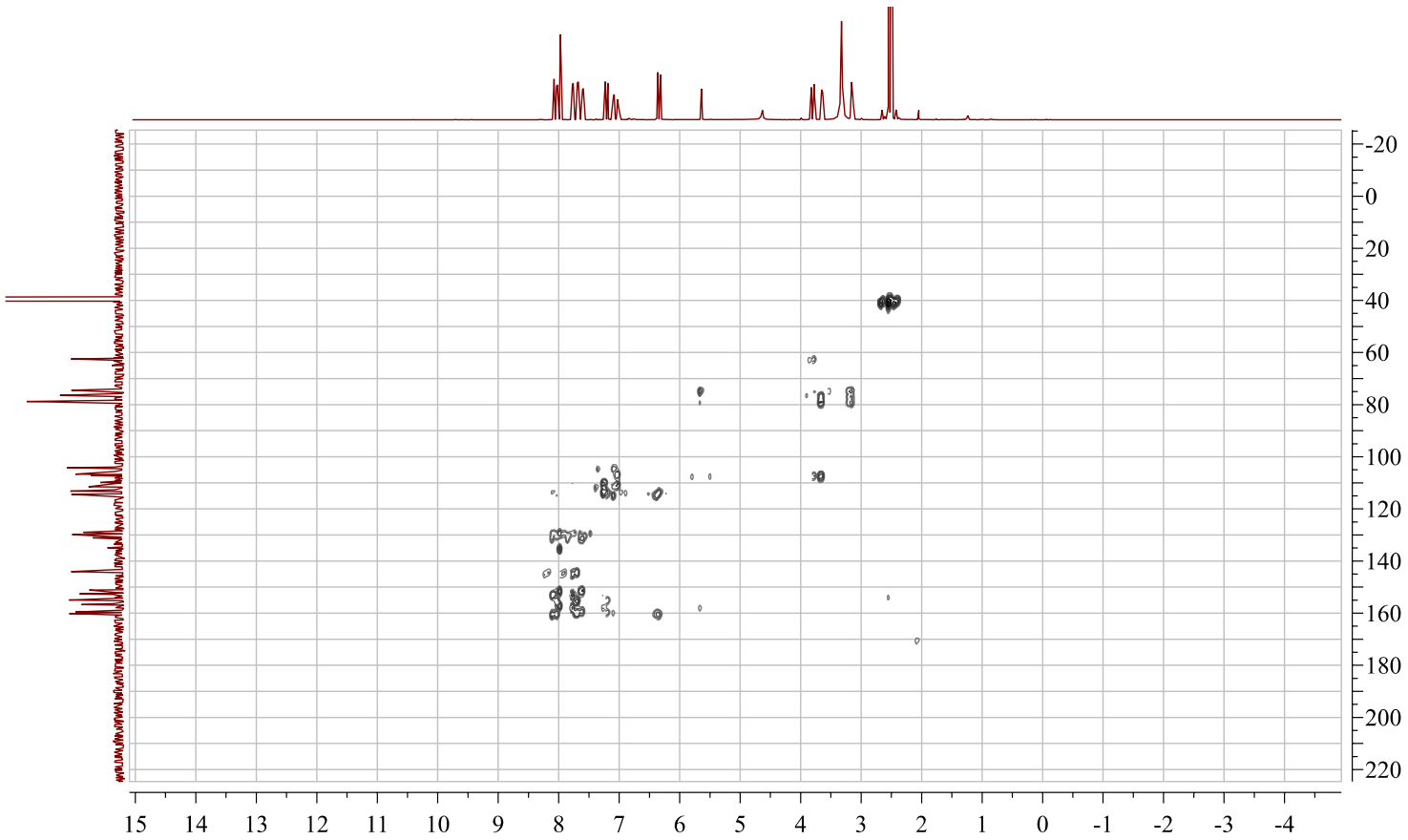

Figure S3. HMBC spectrum of compound **5** in DMSO-d_6

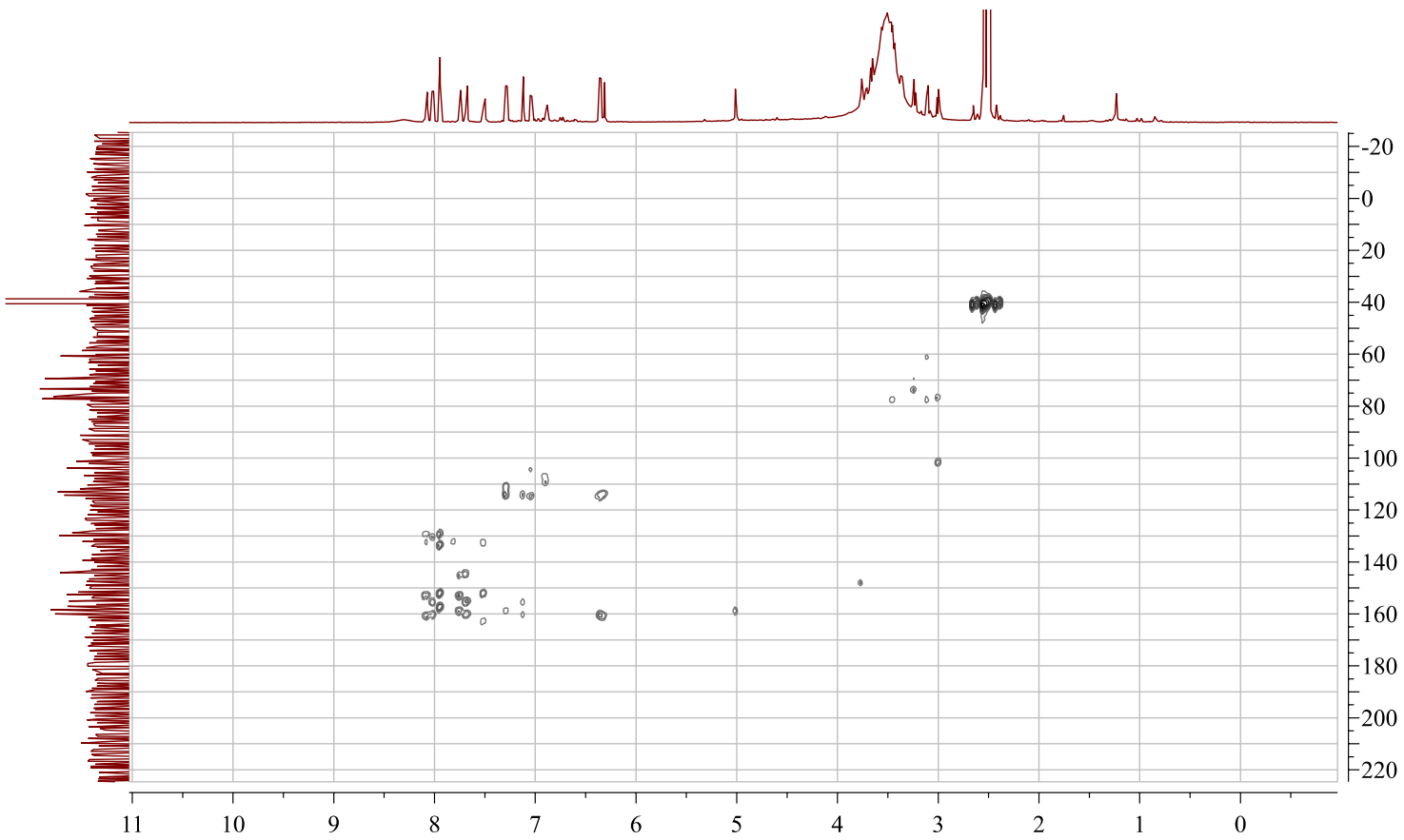

Figure S4. HMBC spectrum of compound **6** in DMSO-d_6

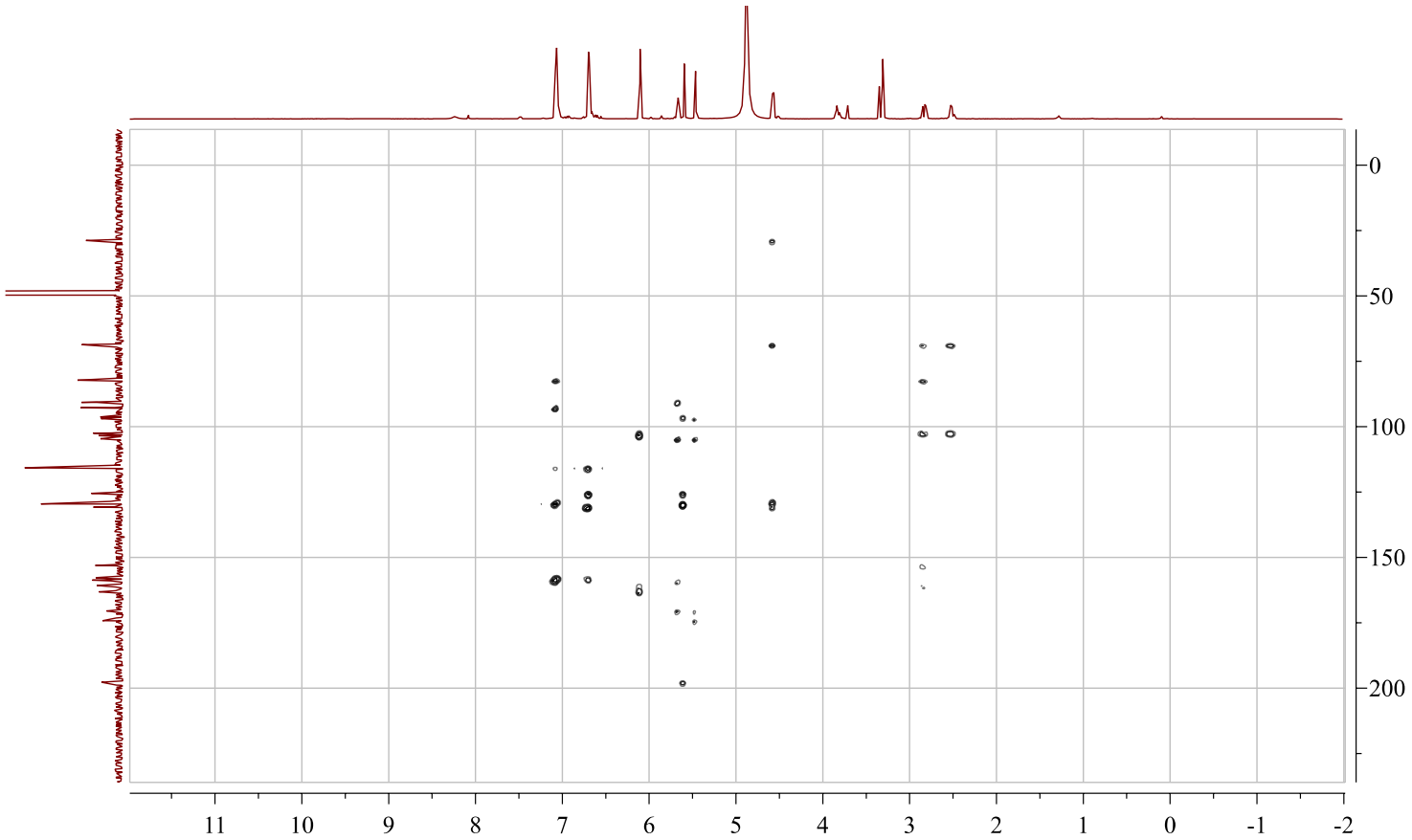

Figure S5. HMBC spectrum of compound **7** in MeOD-d_4